OAK RIDGE NATIONAL LABORATORY LIBRARIES
3 4456 0548501 6

CENTRAL RESEARCH LIBRARY
DOCUMENT COLLECTION

O AL LABORATORY
by
UNION CARBIDE CORPORATION
for the
U.S. ATOMIC ENERGY COMMISSION

ORNL-TM-35

130

CHEMICAL TECHNOLOGY DIVISION

UNIT OPERATIONS SECTION

MONTHLY PROGRESS REPORT

JULY 1961

CENTRAL RESEARCH LIBRARY
DOCUMENT COLLECTION
LIBRARY LOAN COPY
NOT TRANSFER TO ANOTHER PERSON
If you wish someone else to see this document, send in name with document and the library will arrange a loan.

NOTICE

This document contains information of a preliminary nature and was prepared primarily for internal use at the Oak Ridge National Laboratory. It is subject to revision or correction and therefore does not represent a final report. The information is not to be abstracted, reprinted or otherwise given public dissemination without the approval of the ORNL patent branch, Legal and Information Control Department.

LEGAL NOTICE

This report was prepared as an account of Government sponsored work. Neither the United States, nor the Commission, nor any person acting on behalf of the Commission:

A. Makes any warranty or representation, expressed or implied, with respect to the accuracy, completeness, or usefulness of the information contained in this report, or that the use of any information, apparatus, method, or process disclosed in this report may not infringe privately owned rights; or

B. Assumes any liabilities with respect to the use of, or for damages resulting from the use of any information, apparatus, method, or process disclosed in this report.

As used in the above, "person acting on behalf of the Commission" includes any employee or contractor of the Commission, or employee of such contractor, to the extent that such employee or contractor of the Commission, or employee of such contractor prepares, disseminates, or provides access to, any information pursuant to his employment or contract with the Commission, or his employment with such contractor.

ORNL-TM-35

UNIT OPERATIONS SECTION MONTHLY PROGRESS REPORT

July 1961

CHEMICAL TECHNOLOGY DIVISION

M. E. Whatley

P. A. Haas
R. W. Horton
A. D. Ryon
J. C. Suddath
C. D. Watson

Date Issued

JAN 30 1962

OAK RIDGE NATIONAL LABORATORY
Oak Ridge, Tennessee
Operated By
UNION CARBIDE CORPORATION
for the
U. S. Atomic Energy Commission

OAK RIDGE NATIONAL LABORATORY LIBRARIES

3 4456 0548501 6

ABSTRACT

Thoria denitrator products from 0.04 to 0.066 N/Th ratio were dispersed into sols at N/Th ratios of 0.11 to 0.19 and processed by the sol-gel technique to produce final compacted thoria products with little significant variation. Experimental results of H_2-CuO reaction in the helium purification work further substantiated the mathematical model. The elutions of uranyl sulfate loaded Dowex 21K with chloride apparently involved the diffusion of both the sulfate ions and the uranyl ions. The dejacketing of the NaK bonded SRE Core I fuel elements is proceeding satisfactorily with an average rate that has increased to 7 to 8 kg U/hr. The uranium slugs exhibit various degrees of camber and pitting. The disintegration-leaching of 3% U-graphite fuel by flowing 90% HNO_3 at 60°C is apparently superior to a batch-leach method. Attempts to use air bubblers to control the interface level at the bottom of a 2-in.-dia glass pulse column showed considerable loss of pulse amplitude, particularly in taller columns. An air operated diaphragm pump was designed, fabricated, and tested for use as a TrU facility process pump. A successful duplicate test was made calcining TBP-25 waste using the close coupled evaporator-calciner system.

CONTENTS

		Page
	Abstract	2
	Previous Reports in this Series for the Year 1961	4
	Summary	5
1.0	Fuel Cycle Development	7
2.0	GCR Coolant Purification Studies	12
3.0	Ion Exchange	25
4.0	Power Reactor Fuel Processing	27
5.0	Solvent Extraction Studies	33
6.0	Transuranium Element Processing	39
7.0	Waste Processing	44

Previous Reports in this Series for the Year 1961

January	ORNL CF 61-1-27
February	ORNL CF 61-2-65
March	ORNL CF 61-3-67
April	ORNL-TM-32
May	ORNL-TM-33

All previous reports in this series are listed in the June 1961 report, ORNL-TM-34, from the beginning, December 1954.

SUMMARY

1.0 FUEL CYCLE DEVELOPMENT

The dispersion-drying-sintering characteristics were studied for six trough denitrator products of 0.040 to 0.066 N/Th ratio. Particle densities by toluene displacement of the ThO_2 products were 9.77 to 9.86 g/cc relatively independent of sol N/Th ratios of 0.11 to 0.19. Individual particles of up to 3/4-in. maximum dimensions and free of visible cracks under low magnification were obtained from sols of N/Th ratios of 0.11 and 0.14. Sols of N/Th = 0.18 gave much smaller particles with numerous cracks. Crushed samples were compacted by vibration to 8.2 g/cc while ball milled samples compacted to 8.6 or 8.7 g/cc.

A conservative flowsheet was prepared for use by the Sol-Gel Process with virgin $Th(NO_3)_4$ and U-233. Thus, only the steps including uranium require shielding.

2.0 GCR COOLANT PURIFICATION STUDIES

The mass transport factor for gas film diffusion of CO in helium was determined from experimental data to be:

$$J_{D(CO)} = 0.365(Re')^{-0.55}$$

where Re' is the Modified Reynold's Number.

Experimental results of H_2-CuO reaction compare within experimental error with the predicted results based on the model of combined external film diffusion and internal pore diffusion.

3.0 ION EXCHANGE

The rate at which chloride ions elute uranyl sulfate from Dowex 21K has been shown to not be controlled by the counter diffusion of chloride and $UO_2(SO_4)_2^{=}$ ions. It appears likely that the process involves diffusion of chloride ions counter to both sulfate ions and uranyl ions. Because no data on the mobility of uranyl ions in Dowex 21K is available, this mechanism can not be adequately tested. But if the mechanism is assumed, a reasonable value for the uranyl ion self-diffusion coefficient in the resin can be calculated (approximately one-fifth that of the sulfate ion).

4.0 POWER REACTOR FUEL PROCESSING

4.1 SRE Dejacketing Studies

The SRE Core I fuel burned to 675 mwd/ton and decayed ~2 years is currently being dejacketed at the rate of 7 to 8 kg U/hr. This production rate is a factor of ~3 greater than the rate for the first five clusters where an auxiliary dejacketing method was required to slit and pry the jacket from the uranium slugs from 4 of the 34 rods processed. A total of

62 rods have been processed to date. The disposal of the 6 cubic inches of NaK from each fuel rod has progressed satisfactorily in the redesigned disposal unit. Enlarging the NaK transfer lines, rerouting of the nitrogen blanket gas continuous blowdown of reactant steam and isolation of water wash lines have been incorporated. At least 40 batches of NaK have been reacted in the new unit without incident.

All of the uranium slugs have exhibited various degrees of camber and pitting, probably dependent upon their location in the reactor.

4.2 U-C Fuel Processing

Disintegration-leaching of 3% U-graphite fuel by continuous flow of 90% HNO_3 at 60°C confirmed the superiority of this method to a single extended leach or several successive batch leaches. Despite incomplete disintegration, the 3/8-in. fuel cubes were leached to 99.86% U recovery at a flow of 6 gal $ft^{-2}hr^{-1}$ through the 2-in.-dia x 15-in.-high column of graphite. Permeability of the bed was equivalent to that of loose sand - $\sim 10^{-6}$ cm^2.

5.0 SOLVENT EXTRACTION STUDIES

Tests were carried out on two 2-in.-dia glass pulse columns to ascertain the practicability of using an air bubbler system for bottom interface control. Considerable loss of pulse amplitude was observed and the control was very poor and unreliable with the taller column (24 ft) although it seemed satisfactory with the shorter column (12 ft). The effect of air on the flooding characteristics of the 12 ft column was also determined.

6.0 TRANSURANIUM ELEMENT PROCESSING

An air operated diaphragm pump was designed, fabricated, and tested for use as a TrU facility process pump. Satisfactory operation for a suction of 13.5 ft was demonstrated with saturated LiCl solution. The design permits remote replacement of the pumps or check valves on a mounting rack and provides complete containment of the operating air.

7.0 WASTE PROCESSING

A duplicate test of the close coupled evaporator-calciner operation using Idaho type waste (TBP-25) was made under nearly identical conditions as the last test reported previously. The calcined solids had a bulk density of 0.56 g/cc and retained 77% of the ruthenium added with the feed. Only 2% of the mercury remained in the solids with the bulk of the mercury being accumulated in the evaporator. There was no excessive corrosion on either side of the pot wall by visual observation.

1.0 FUEL CYCLE DEVELOPMENT

P. A. Haas

The fuel cycle program is a study of fuel materials preparation and element fabrication procedures economically adaptable to remote operation for the recycle of fissile and fertile materials. The immediate objective is to develop to the pilot plant stage the process for ThO_2-U(233)O_2 in cladding tubes. The Unit Operations studies are on denitration of $Th(NO_3)_4$ in steam atmospheres followed by dispersion into thoria sols, uranium addition, drying, and calcination to give high density oxide particles. Test elements of vibratorily compacted oxides are being fabricated or irradiated.

1.1 Dispersion-Drying-Calcining Studies - C. C. Haws, Jr., R. D. Arthur

Dispersion characteristics and their effect upon density, vibratory compaction and shard size of the six repetitive denitrator batches (June Unit Operations monthly report) were studied. Samples taken from the six batches were dispersed, one from each run at N/Th ratios of 0.11, 0.14, and 0.18. The average shard densities obtained from each of the three series of six samples were: 9.82 (σ = 0.03), 9.77 (σ = 0.04), and 9.86 (σ = 0.05) g/cc, respectively. Vibratory compaction densities obtained on ten samples in which size reduction was obtained by pulverizing were ~8.2 g/cc. Compaction densities of two samples reduced by ball milling were 8.7 (N/Th = 0.16) and 8.6 (N/Th = 0.12) g/cc. The shards produced from the 0.11 and 0.14 sols were large and almost crack-free. Individual shards could be selected in which the largest dimension was 3/4-in. and in which no cracks were visible under the microscope. The 0.18 sols yielded shards only a fraction as large as those from the lower N/Th sols and these were highly cracked. Size reduction of this material would not yield the required minimum 65 wt % of +16 mesh fragments.

The mechanism by which ball milling permits an increase in vibratory compaction density is not known. Perhaps the low densities obtained in absence of ball milling results from an electrostatic phenomenon, from surface condition and/or shape of the thoria shard, from the filling of very fine cracks by fines produced and placed in location by the ball mill, or from combinations of these. To observe these variables, a 100 g sample of 10/16 mesh shards was tumbled overnight in 14 N nitric acid for the purpose of etching the surface of the shards, rounding of sharp edges and corners, and for removing any fines held electrostatically to the fragments. The fragments emerging from this treatment were much more rounded than is normally obtained in dry ball milling. Surfaces were etched, having a sand blasted appearance. The sample, when recombined and vibrated, gave a density of ~8.0 g/cc compared with ~8.2 g/cc before treatment. The toluene density of the sample was 9.77 g/cc, not significantly below its original toluene density.

These observations indicate that the presence of sharp corners and edges (the "shape factor") along with highly polished surfaces of an electrostatic effect may not be deleterious since removal of these two conditions actually caused a decrease in the compacted density.

1.2 Sol-Gel Process Flowsheet - J. W. Snider, C. C. Haws, Jr.

The development of the Sol-Gel Process has progressed to the state that a workable flowsheet can be drawn. This conservative flowsheet may not be optimum for the final process; several items are included which subsequent development work may eliminate or simplify. The equipment included should accommodate any modification envisioned at the present.

The attached flowsheet (Figures 1.1 and 1.2) includes estimates of the flow rates, equipment sizes and times per batch as a guide in designing the Sol-Gel Process for a 4 ton/year (13.8 kg/work day) ThO_2 plant. The batch size was chosen as 66.3 lb (30 kg) thorium nitrate per batch. The flowsheet is proposed for virgin $Th(NO_3)_4$ to be used for U-233 and its accompanying radiation problems.

All steps mentioned through the thorium inventory control would not require remote operation if virgin Th is used. However, if the long range problem is considered, these steps will require shielding also. For this flowsheet, virgin Th is considered and only the steps including uranium require shielding.

There are unresolved alternates which are included, and a list of the major unresolved questions and suggested lines of consideration in the absence of development data are discussed. Future process development is expected to answer these questions.

1. Calciner. What batch size and steam flow rate are desirable? It is possible that the batch size may be doubled. An average of 4.6 batches per week will be required at the proposed batch size to give the proposed throughput.

2. Calciner. Is an air firing step after steam denitration required? If air firing is necessary, there are two proposed alternates.

A. The calciner can be purged with air while at temperatures up to 500°C for about 2 hrs following the steam step.

B. If a temperature over 700°C is required an additional air firing furnace is necessary with another transfer of powdery material.

3. Sol Preparation Tank. What method of agitation is required? An inverted cone with a centrifugal pump or standard portable agitators may suffice. Dispersion in the calciner by addition of water may be feasible. Actual operation of prototypes will be required. Addition of powder to agitated water has been more effective than addition of H_2O to powder.

4. Sol Storage and Aging. What is the most convenient acceptable sol storage and aging procedure? It appears desirable to have a large holdup volume, sufficient for 4 - 6 weeks' inventory, in which the sol may be aged and tested. This point in the flowsheet allows the independent selection of the batch size for the remainder of the flowsheet, with criticality and convenience in mind.

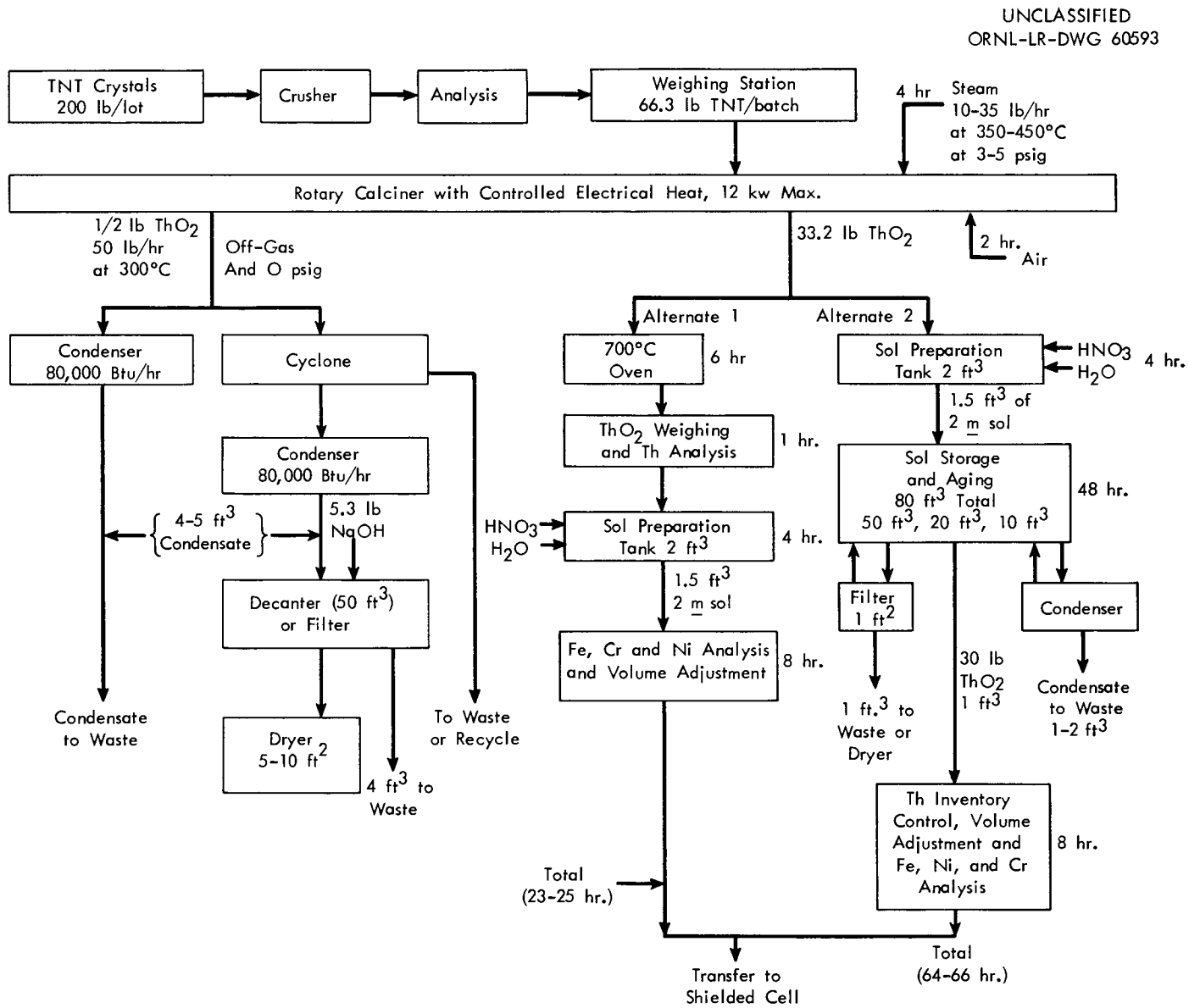

Fig. 1.1. Sol-gel process flow sheet for cold laboratory operation.

UNCLASSIFIED
ORNL-LR-DWG 60594

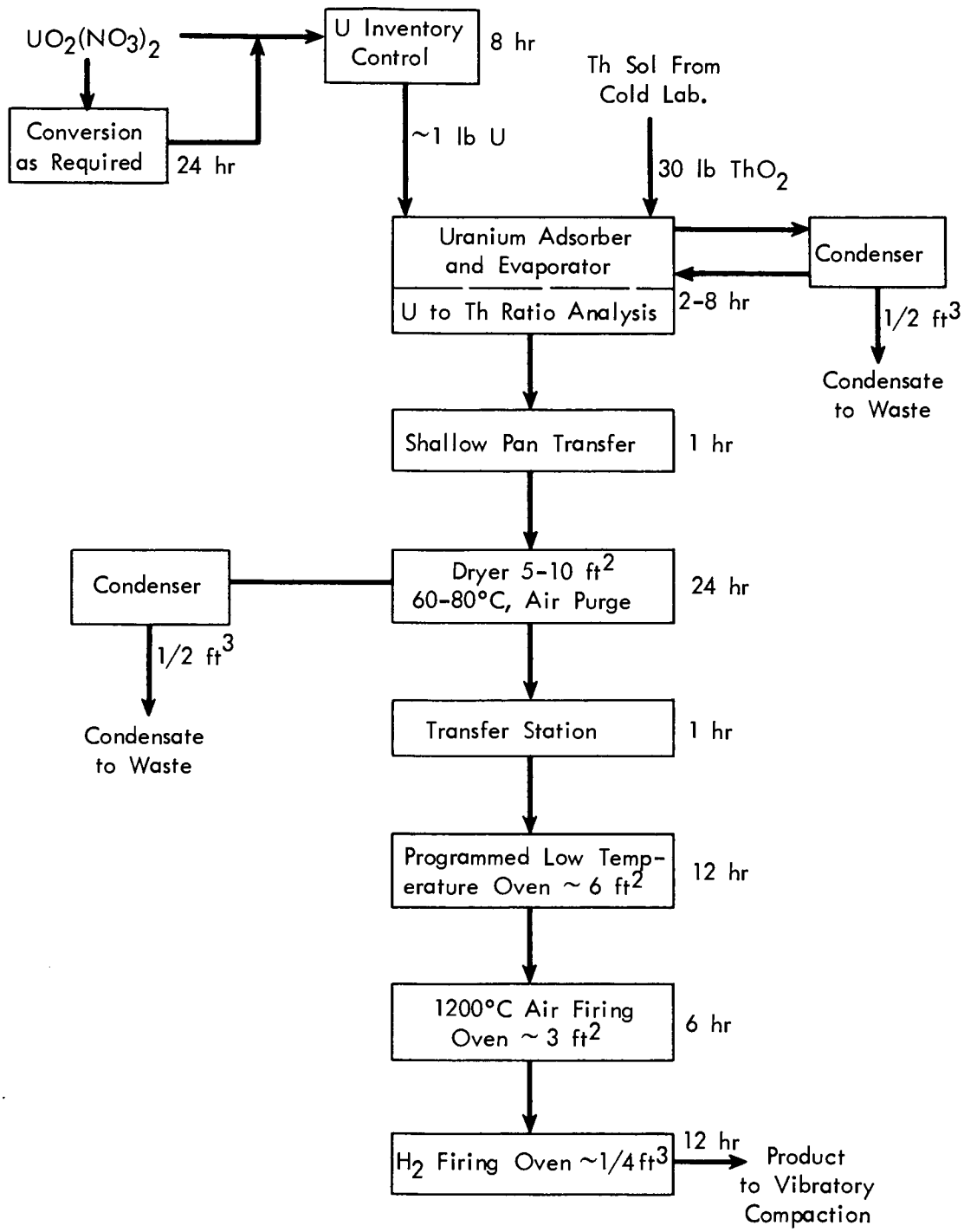

Fig. 1.2. Sol-gel process flow sheet for hot cell operation.

5. Th Inventory Control. What procedure is necessary to ensure transfer of controlled amounts of good sol to the remotely operated part of the facility? This step in the flowsheet may not be required if a large holdup of inventory in the prior step is allowed. However, if a large holdup is not permitted, this step is necessary for analysis and concentration adjustment.

6. Uranium Conversion. Is conversion of uranyl nitrate to another form required? The final answer to this question will require experimental study. The flowsheet allows for ADU precipitation.

7. Firing. What maximum pan depth may be used for firing the post dried sol-gel product? Present indications are that trays more than 1 inch deep shall be required.

8. Firing. Can the product be held at 500°C for a length of time prior to the 1200°C plunge? If this is permitted it may allow a reduction in the number of low-temperature furnaces required and a much less tedious programming of various steps.

9. Firing. What length of soak time is required under H_2 and what cool-down procedure should be used?

10. Firing. What type and size of furnaces are best suited for remote operation? From cost, ease of handling, maintenance, and operational flexibility, small muffle and globar furnaces are attractive. Eight low-temperature (500°C) muffle furnaces and four 1200°C furnaces of the type used in development studies would meet production schedules and can be purchased with two programmed controllers for ~$7,500. A larger number of transfers behind shielding would be required because of the smaller batch sizes, but larger batches and trays would be more difficult to handle remotely.

11. Firing. Is it necessary to cool the air fired product to room temperature prior to H_2 firing? Consultation with personnel of the Metallurgy Division indicates that cooling may be desirable.

Other possible process improvements or simplifications dependent on development studies include:

1. Use of $Th(NO_3)_4$ solutions or molten salt as a feed to avoid handling the solid salt.

2. The recycle to the calciner of thoria removed from the calciner off-gas by a cyclone.

3. Improved decantation or filtration procedures to minimize the thoria lost with the undispersed heel.

2.0 GCR COOLANT PURIFICATION STUDIES

J. C. Suddath

Contamination of coolant gases by chemical impurities and release of fission products from fuel elements are major problems in gas cooled reactors and in-pile experimental loops. Investigations are being made to determine the best methods to reduce the impurities, both radioactive and non-radioactive with emphasis on the kinetics of the fixed bed oxidation of hydrogen, carbon monoxide, and methane by copper oxide.

An attempt is being made to fit experimental data from the study of the H_2-CuO and CO-CuO reactions to a mathematical model of external diffusion and internal diffusion of the H_2 or CO controlling a rapid, irreversible reaction.

2.1 Determination of Apparent Mass Transfer Factors - C. D. Scott

The mass transfer factor, J_D, for H_2 transport across an assumed gas film was previously determined for all of the deep bed kinetic tests for the H_2-CuO reaction ($H_2 + CuO \rightarrow H_2O + Cu$)(Unit Operations Monthly Report, June 1961). The expression for the mass transfer factor for H_2 transport as a function of Modified Reynold's Number was,

$$J_{D(H)} = 0.24(Re')^{-0.69} \qquad (1)$$

where,

$J_{D(H)}$ = mass transfer factor for H_2 transport, dimensionless

Re' = Modified Reynold's Number, dimensionless

The same procedure was used to determine the mass transfer factor for the transport of CO from a flowing stream of helium to CuO pellets. The values for J_D for CO transport are shown in Figure 2.1. The resulting expression for the least squares fitted curve was:

$$J_{D(CO)} = 0.365(Re')^{-0.55} \qquad (2)$$

These values of J_D for CO transport are somewhat higher than the values of J_D for H_2 transport.

2.2 Comparison Between Predicted Results and Experimental Data from Deep Bed Kinetic Tests

The method used to test the mathematical model with experimental data for the H_2-CuO reaction was to use the model to predict results which could be measured experimentally. The finite difference solution of three differential equations which described the system mathematically was used to predict effluent H_2 concentration history curves (Unit Operations Monthly Report, May 1961). These predicted curves were then compared to experimental curves.

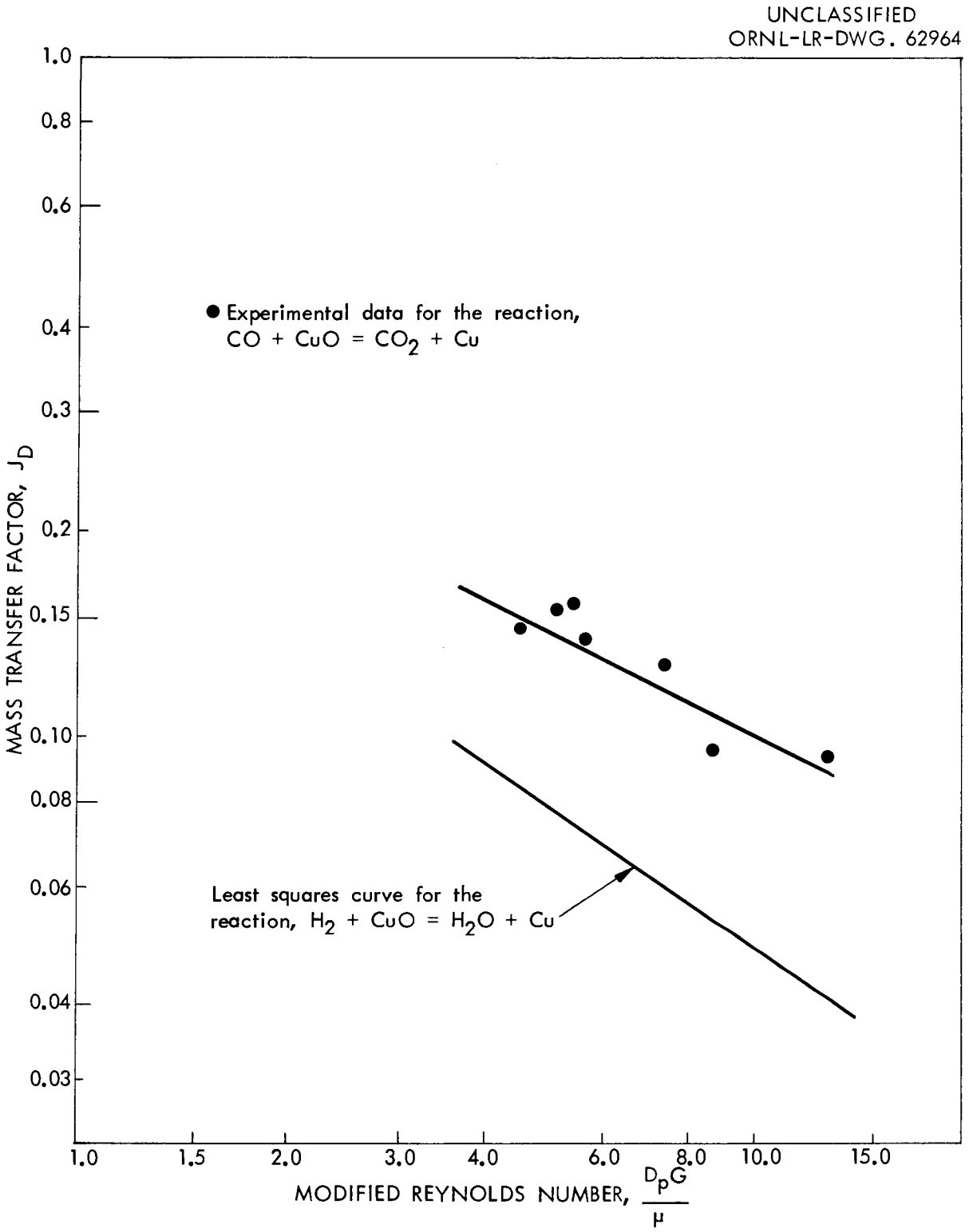

Fig. 2.1. Mass transfer factor as a function of modified Reynolds number for the reaction, $CO + CuO = CO_2 + Cu$, compared with the mass transfer factor for the reaction, $H_2 + CuO = H_2O + Cu$.

A total of 24 deep bed tests (Unit Operations Monthly Report, May 1961) were used to compare predicted results with experimental results (Figures 2.2 to 2.10). The tests cover the following ranges of operating conditions:

System pressure - 10.2 - 30.0 atm
System temperature - 400 - 600°C
Gas mass flow rate - 0.072 - 0.255 g-moles/cm^2-min
H_2 concentration in helium stream - 0.097 - 1.20 vol %
CuO pellet bed volume - 24 - 192 cc

The experimental results compare within experimental error to the predicted results except in some cases for the initial and final parts of the curves (Figures 2.2 to 2.10). The effects of experimental error can be shown for run R-3 in which the experimental curve was displaced from the predicted curve in the latter part of the run. However, the experimental curve generally fell within the range of predicted values when the possible experimental error of $\pm$ 5% for the initial H_2 concentration and $\pm$ 5% for the total gas flow rate was considered (Figure 2.11).

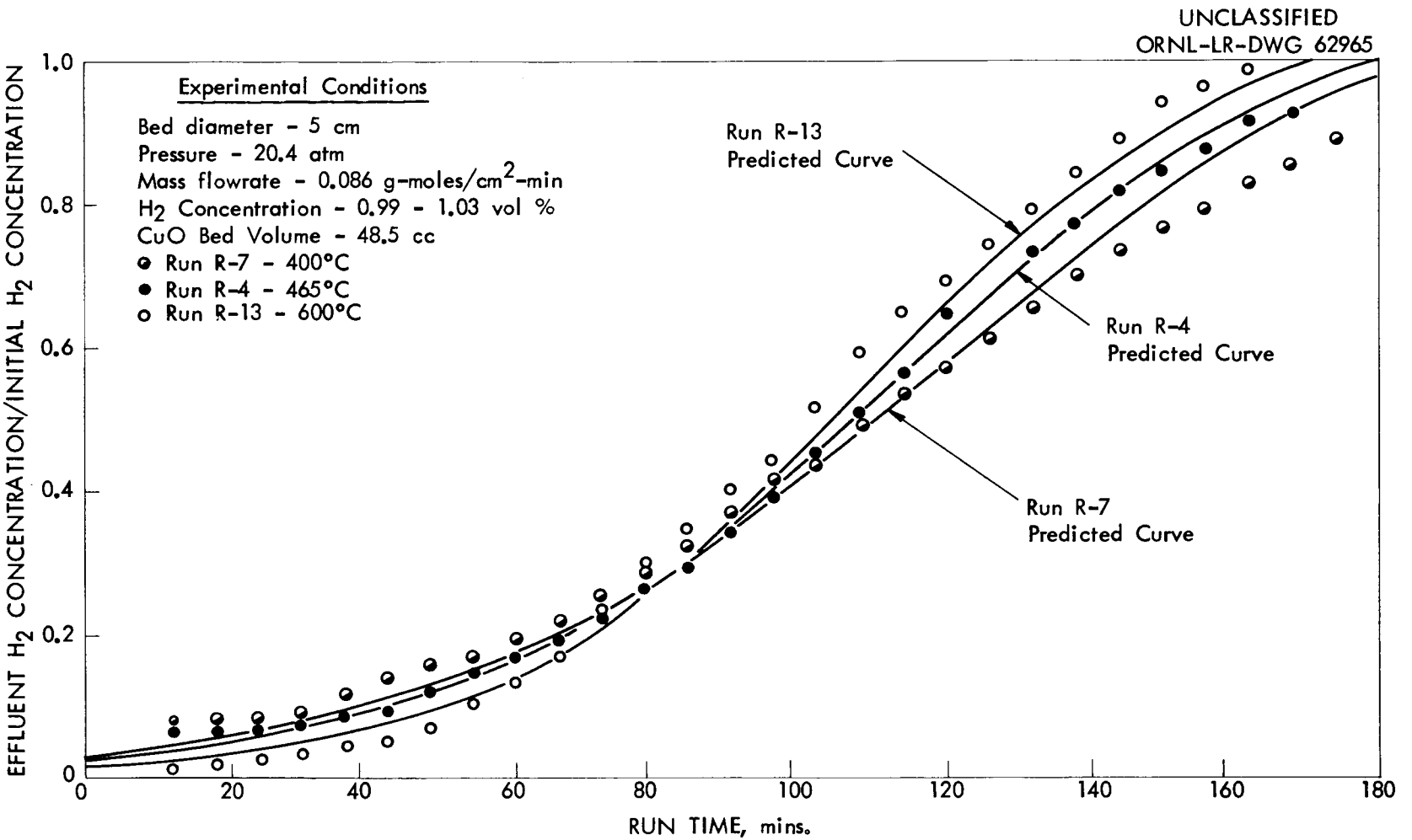

Fig. 2.2. Effect of temperature on the effluent H_2 concentration history curve for the reaction of hydrogen in a flowing stream of helium with a fixed bed of porous CuO pellets.

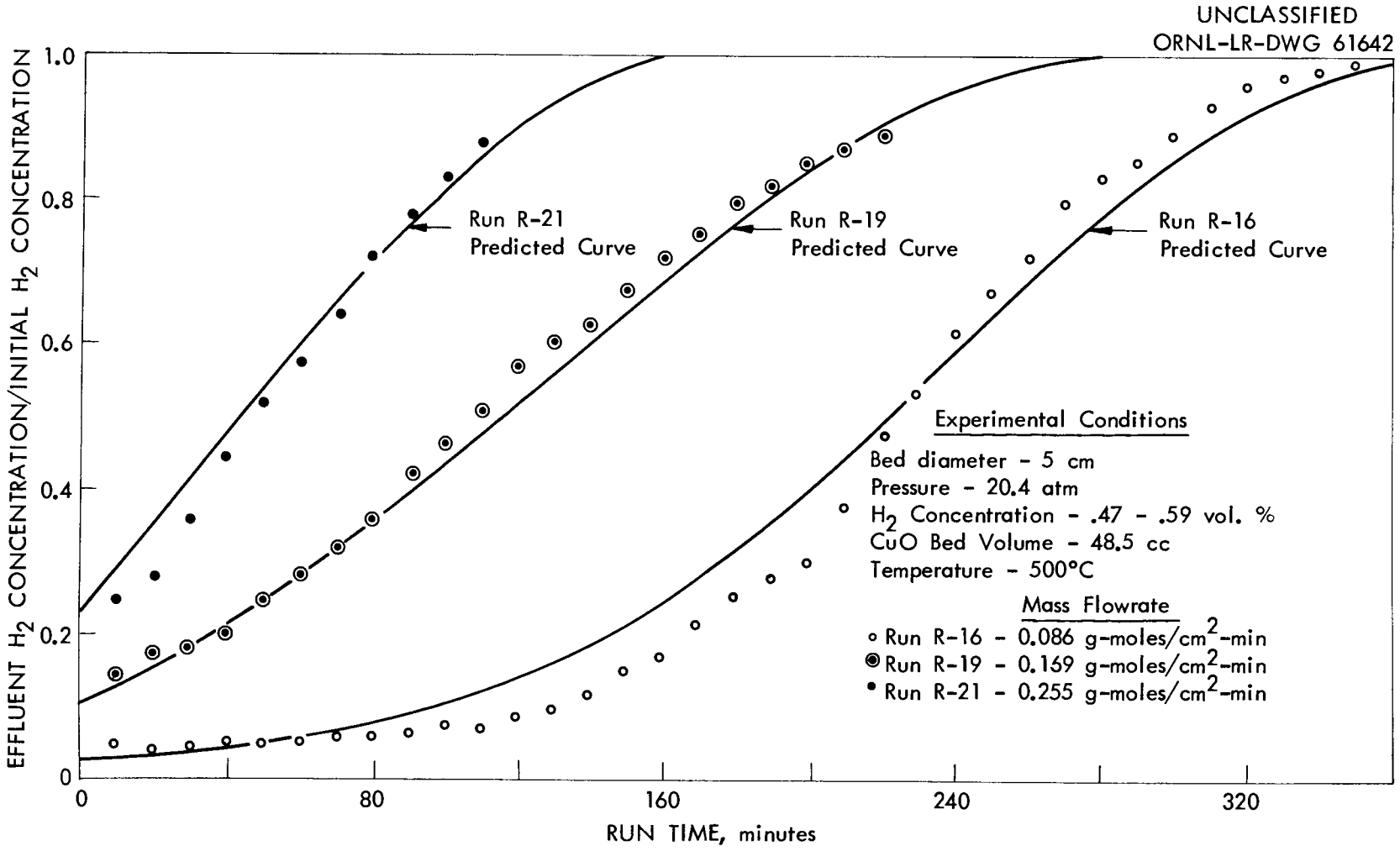

Fig. 2.3. Effect of mass flowrate on the effluent H_2 concentration history curve for the reaction of hydrogen in a flowing stream of helium with a fixed bed of porous CuO pellets.

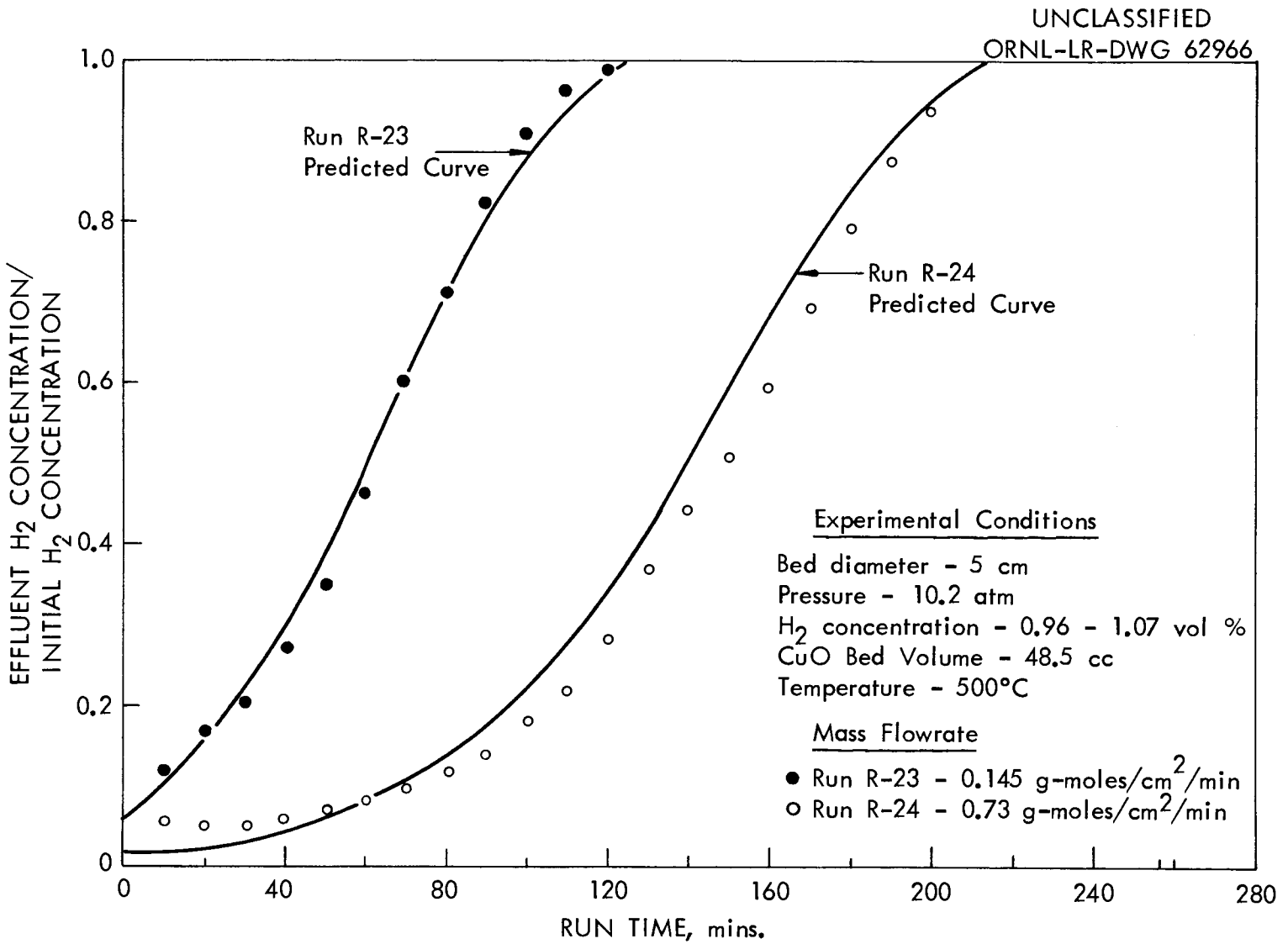

Fig. 2.4. Effect of mass flowrate on the effluent H_2 concentration history curve for the reaction of hydrogen in a flowing stream of helium with a fixed bed of porous CuO pellets.

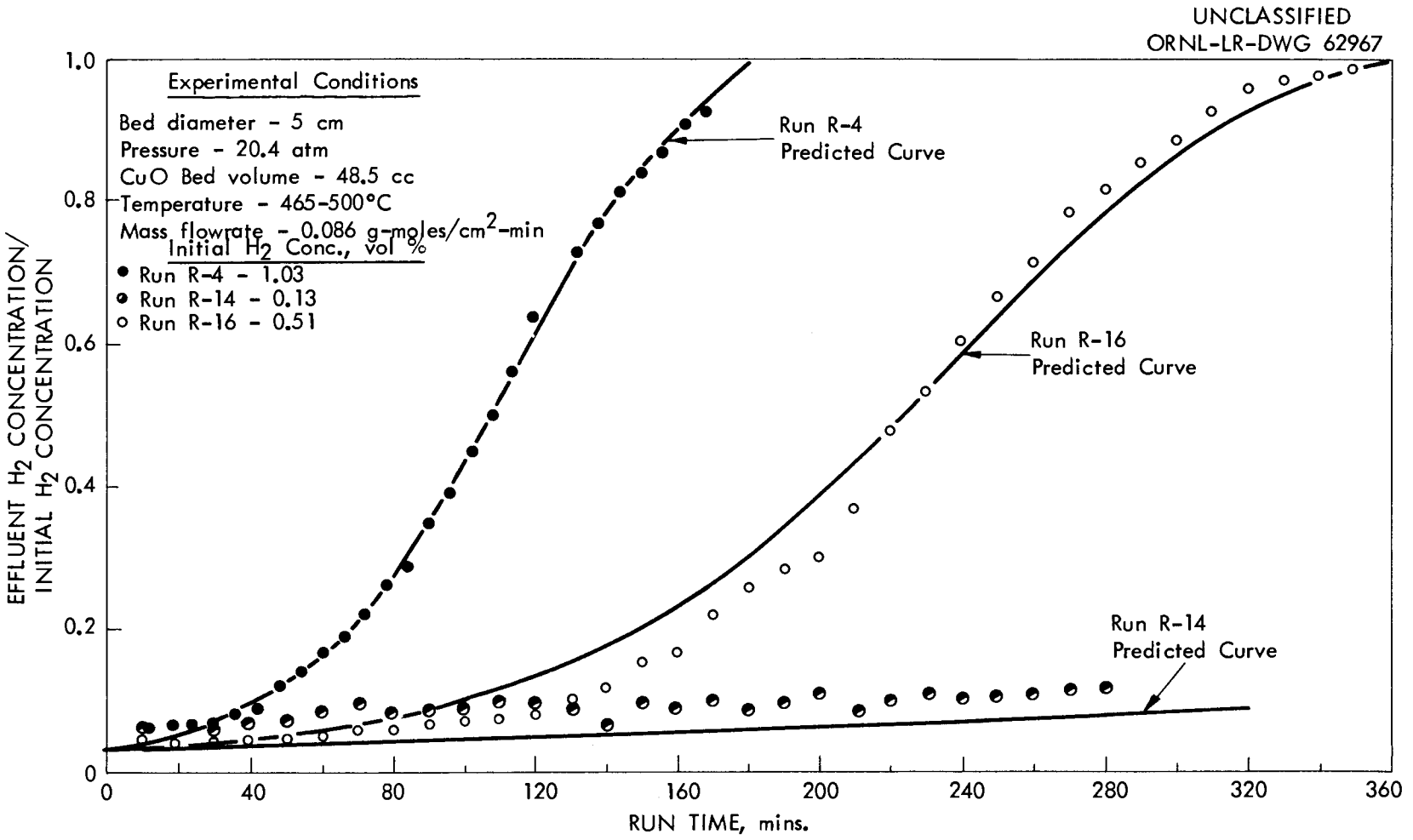

Fig. 2.5. Effect of initial hydrogen concentration on the effluent H_2 concentration history curve for the reaction of hydrogen in a flowing stream of helium with a fixed bed of porous CuO pellets.

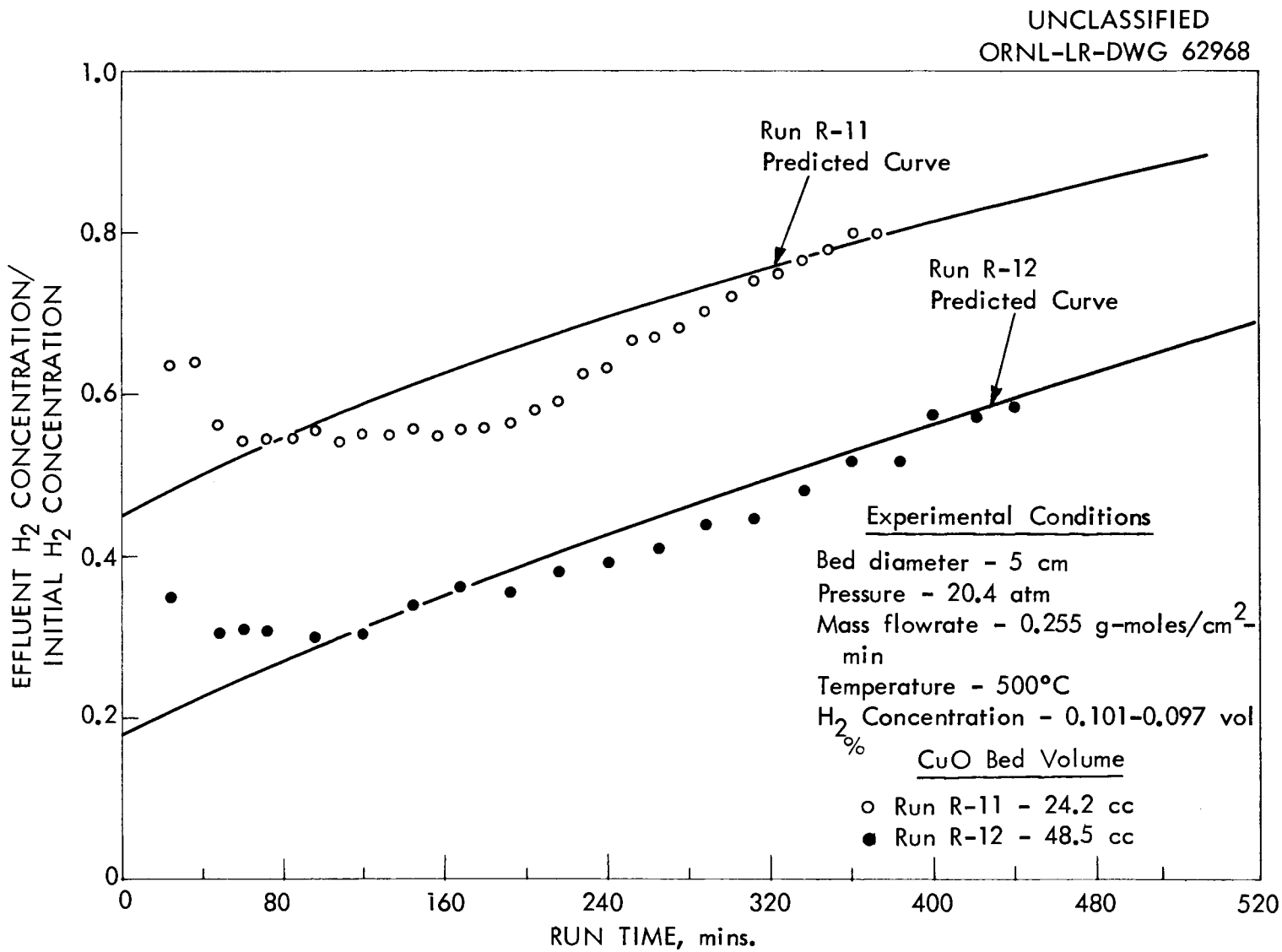

Fig. 2.6. Effect of CuO bed volume on the effluent H_2 concentration history curve for the reaction of hydrogen in a flowing stream of helium with a fixed bed of porous CuO pellets.

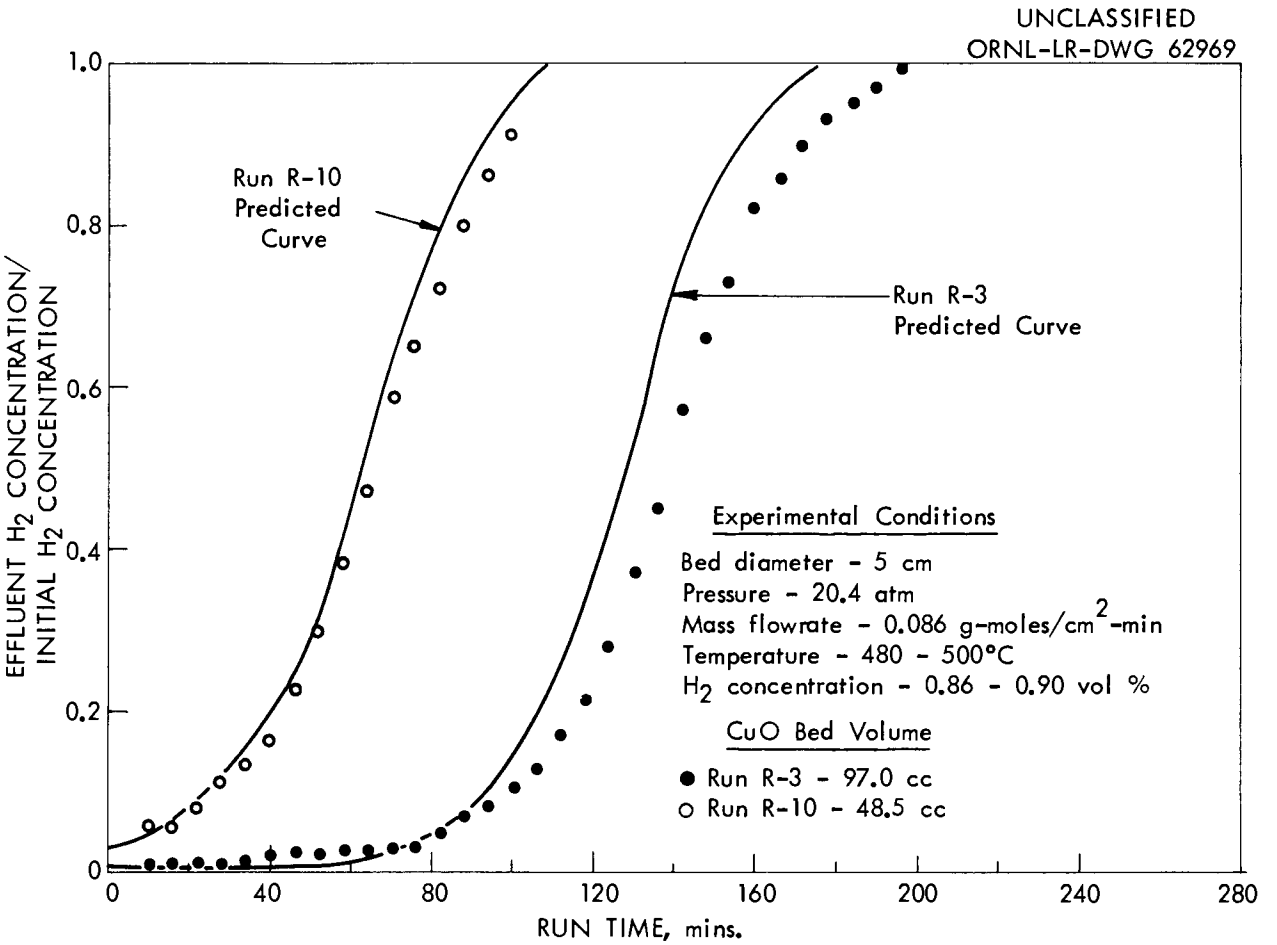

Fig. 2.7. Effect of CuO bed volume on the effluent H_2 concentration history curve for the reaction of hydrogen in a flowing stream of helium with a fixed bed of porous CuO pellets.

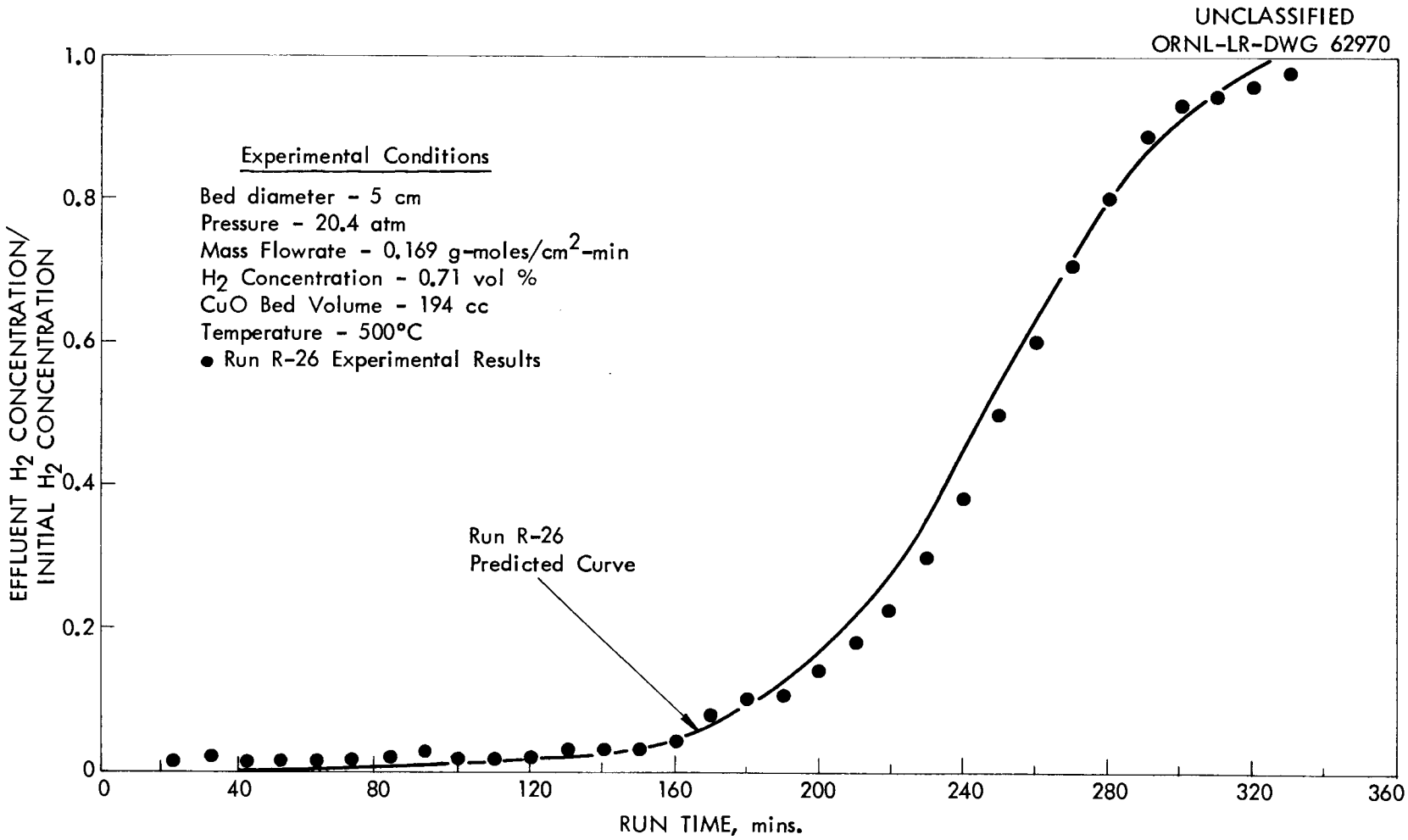

Fig. 2.8. Effluent hydrogen concentration history curve for Run R-26 made at maximum system volume of 194 cc of CuO fixed bed.

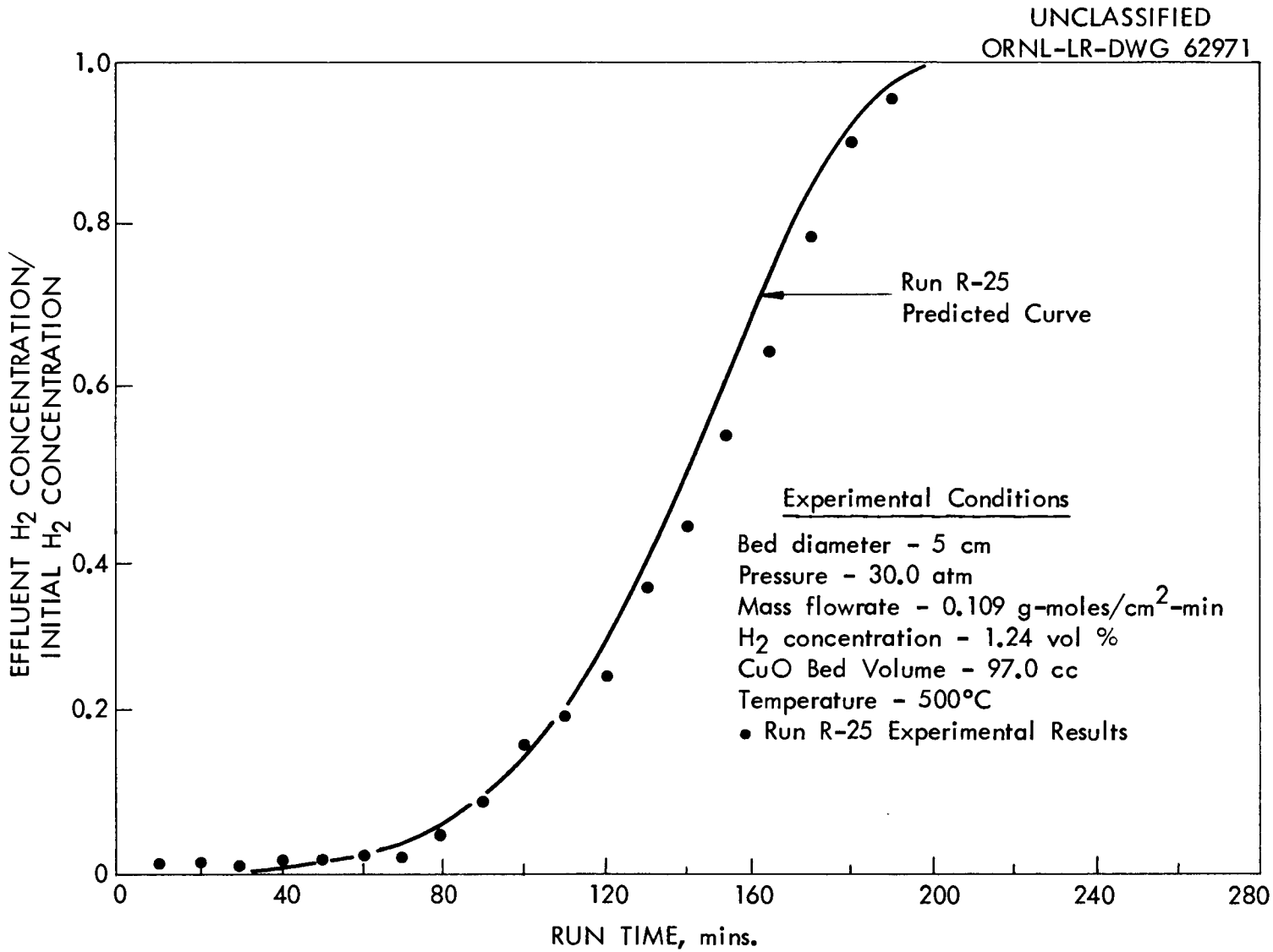

Fig. 2.9. Effluent hydrogen concentration history curve for Run R-25 made at maximum system pressure of 30.0 atm.

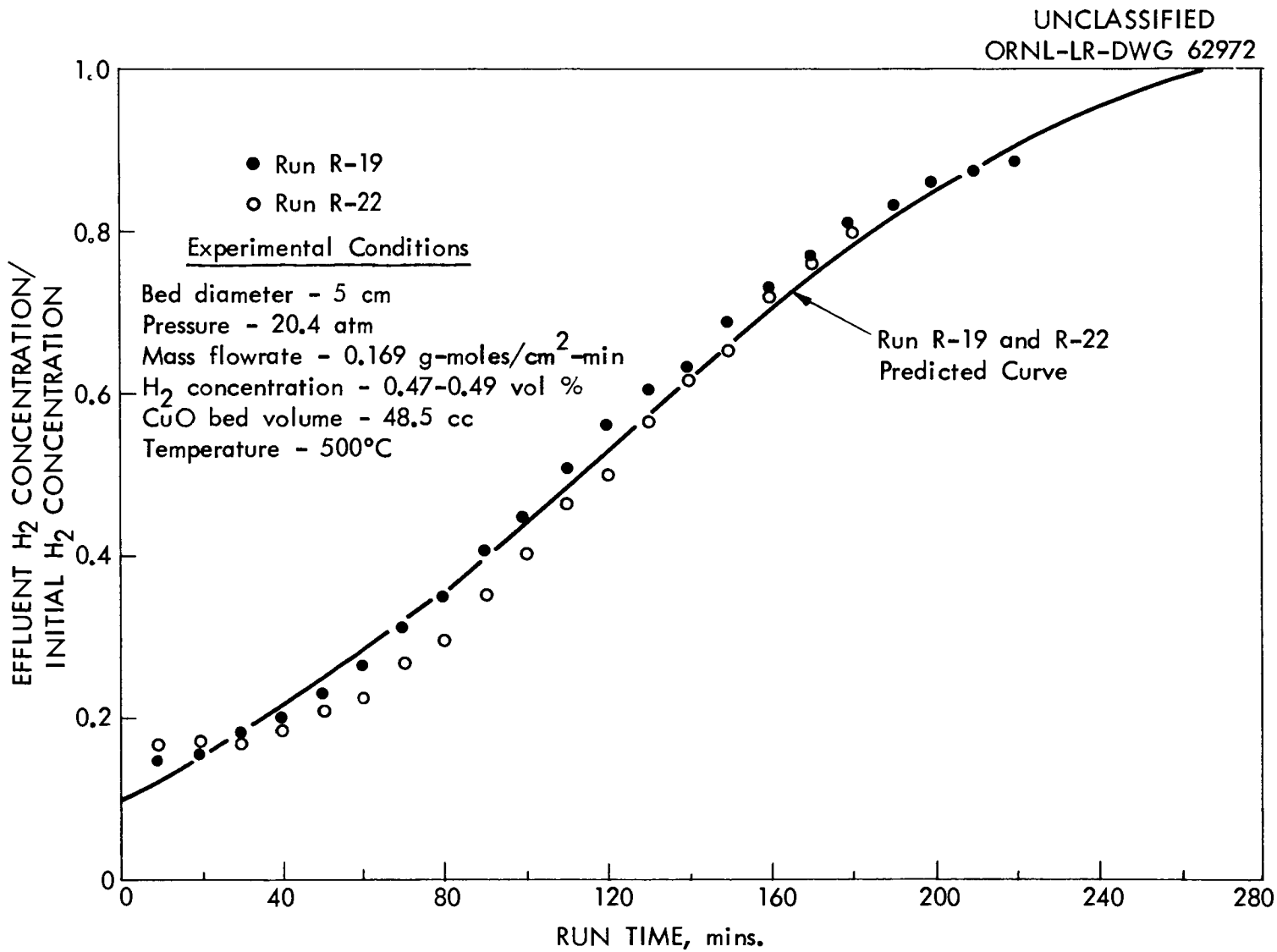

Fig. 2.10. Effluent hydrogen concentration history curves for Runs R-19 and R-22 showing reproducibility of the experimental system.

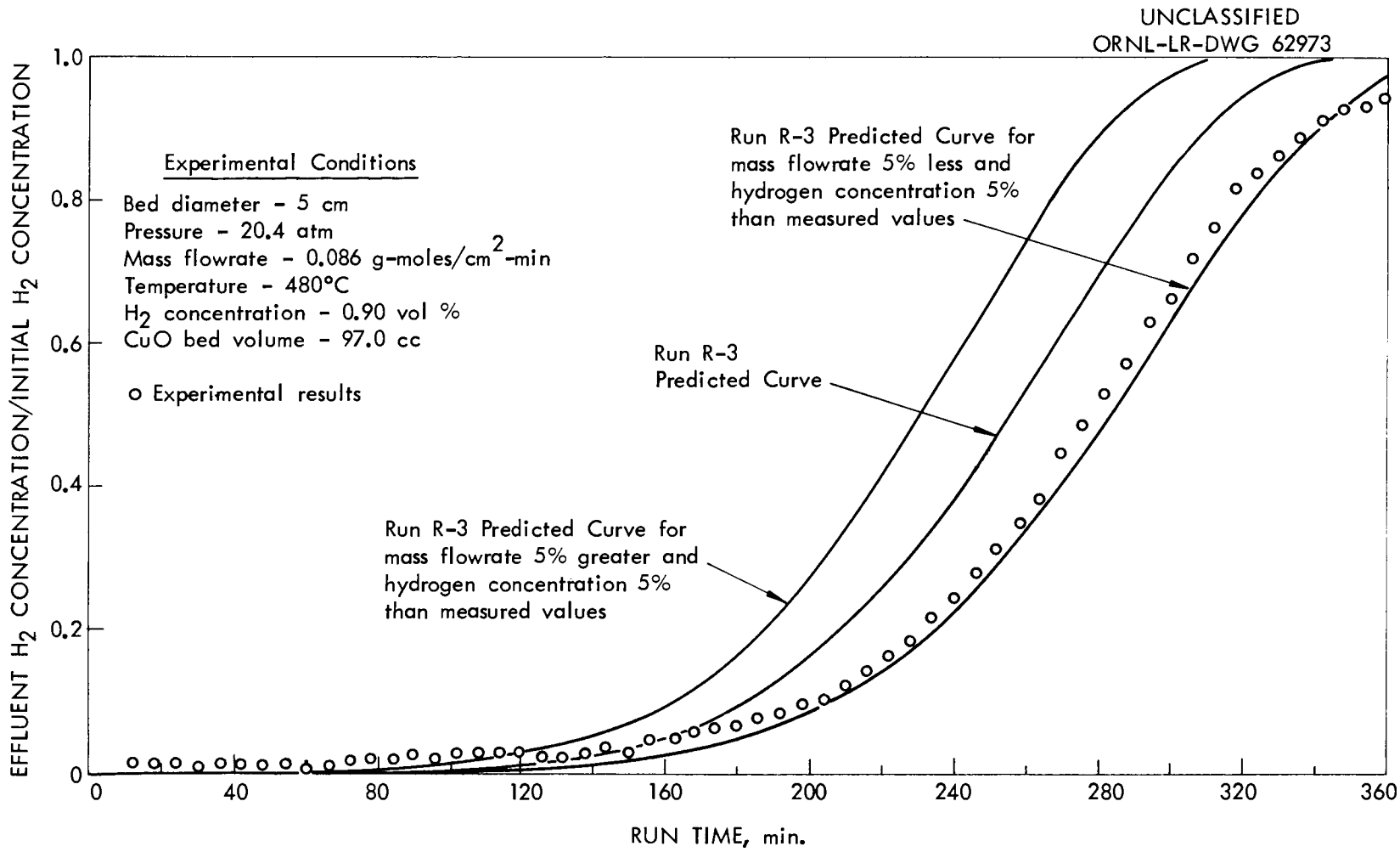

Fig. 2.11. Effect of experimental error on the effluent hydrogen concentration history curve for Run R-3.

3.0 ION EXCHANGE

J. C. Suddath

To make rational predictions of the operating characteristics of uranium anion exchange contactors, an understanding of the mechanism and kinetics of the exchange is necessary. Toward this objective the equilibrium sorption isotherms and rates of sorption of uranium on Dowex 21K are being determined.

3.1 Chloride Elution of Uranyl Sulfate Equilibrated Resin - J. S. Watson

Application of the same analytical techniques used to study uranyl sulfate loading rates on chloride and sulfate equilibrated Dowex 21K has not been as completely successful in predicting the uranyl sulfate elution rates and determining the ions involved. However, this trouble was anticipated. In the loading studies, the exchange rate was found to be satisfactorily predicted by calculating from the self-diffusion coefficients of the ions the rates at which sulfate and/or chloride ions will exchange with $UO_2(SO_4)_2^{=}$ ions. The uranium appeared to exist predominantly as the highly complexed $UO_2(SO_4)_2^{=}$ ion even during loading on chloride equilibrated resin. This results from the extremely low mobility of the $UO_2(SO_4)_2^{=}$ ion when compared with those of the sulfate and chloride ions. During loading, the chloride ions are displaced by sulfate and $UO_2(SO_4)_2^{=}$ ions whose "fronts" move into the resin. However, because the sulfate ions are so much more mobile, the sulfate "front" moves much more rapidly and the uranium is always in the presence of a relatively high sulfate concentration and would be expected to be highly complexed.

During elution, however, the situation is considerably different. In this case the uranium "front" lies in a region where the chloride concentration is high and the sulfate concentration low. Under these conditions one would not expect the elution rates to be controlled by diffusion of the $UO_2(SO_4)_2^{=}$ ion. Curve A in Figure 3.1 shows that the elution rates can not be adequately predicted by calculating the rate at which chloride ions counter diffuse into a resin equilibrated with $UO_2(SO_4)_2^{=}$.

Because of the low sulfate concentration around the uranium "front" one would suspect that the elution rates could be predicted by calculating the rate at which chloride ions will diffuse into a resin occupied with UO_2^{++} and sulfate ions. There is one drawback to this hypothesis. There is no method for accurately measuring the self-diffusion coefficient of the uranyl ion within the resin to test its validity. However, two sets of calculations have been made using assumed values for the uranyl ion self-diffusion coefficient. First it was assumed to have the same coefficient in 960 micron Dowex 21K as the $UO_2(SO_4)_2^{=}$ ion, and then it was assumed to have a coefficient ten times greater. The results of these calculations are shown in Curves B and C in Figure 3.1. Note that the later assumption gave a much better fit of the data. These results really prove nothing, but they show the reasonableness of the hypothesis. One would expect the mobility of UO_2^{++} to be greater than $UO_2(SO_4)_2^{=}$ and value assumed to calculate Curve C is not reasonable. Here the UO_2^{++} ion is still considered to be only approximately 1/5 as mobile as the sulfate ion and 1/15 as mobile as the chloride ion in the resin.

UNCLASSIFIED
ORNL-LR-DWG 62974

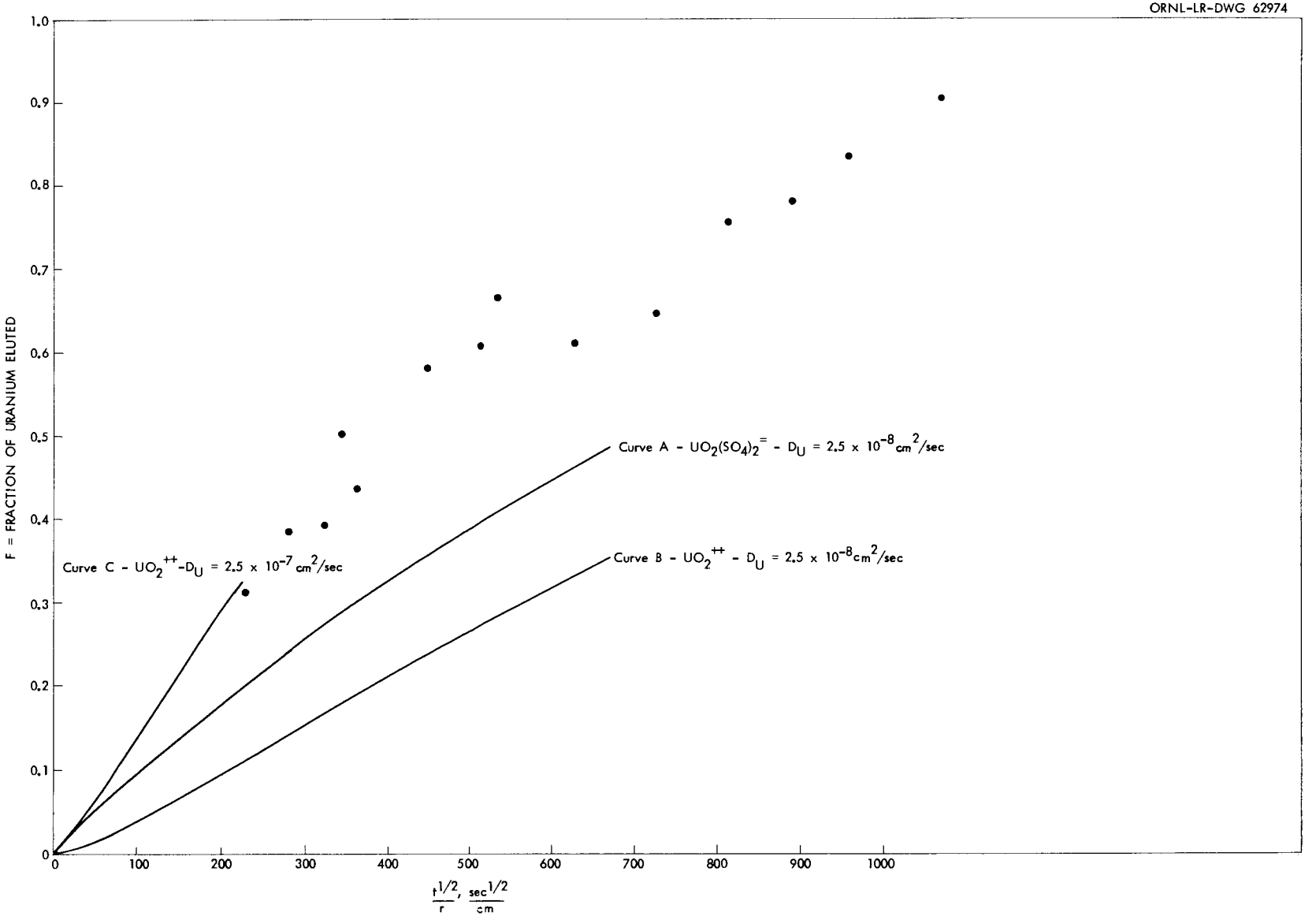

Fig. 3.1. Measured and claculated uranyl sulfate elution rates.

4.0 POWER REACTOR FUEL PROCESSING

C. D. Watson

4.1 SRE Dejacketing Studies - G. A. West

Mechanical dejacketing techniques are being demonstrated in the ORNL High Level Segmenting Facility, Bldg. 3026-D, by processing NaK bonded, stainless steel clad uranium fuel from the Sodium Reactor Experiment, Core I, burned to 675 mwd/ton and decayed ~2 years.

The first carrier load of SRE fuel, 9-6/7 clusters (normally 7 rods per cluster), containing ~680 kg U was processed at a maximum rate of 8.9 kg U/hr. The average rate for the last five clusters was 7.8 kg U/hr after equipment changes and operational techniques were familiarized; the rate on the initial five clusters was 2 to 3 kg U/hr. This lower production rate was mainly due to difficulty in dejacketing five fuel rods apparently damaged by the high heat excursion in the reactor. Auxiliary dejacketing of these rods required the cutting of each fuel rod into twelve fuel slugs, 6 inches long, and the slitting of each slug length longitudinally by an auxiliary dejacketing die containing two sharp-edged rotary disc cutters. The slit jacket was then pryed from each uranium slug. There were three methods used to dejacket the 69 fuel rods mechanically processed. Following removal of the end caps (1) the slugs from 23 fuel rods were hydraulically flushed from the tubular jacket, (2) the slugs from 41 fuel rods were dislodged by a jackscrew traversing internally through the length of the 92-in. long tubular fuel jacket, and (3) five fuel rods were slit open.

The mechanically dejacketing of SRE Core I fuel has not proceeded as rapidly as planned (10-20 kg/hr) because the stainless steel jackets of the spent fuel are not ductile as expected and do not expand with internal hydraulic applied pressures of up to 2700 psig. Normally the jackets of unirradiated prototype fuels would expand at an internal pressure of 1850 psig as much as 380 mils, bursting at slightly higher pressures. The embrittlement of the SRE Core I jackets and loss of ductility is a totally unexpected development. Measurements made by Atomics International[1] show little or no carburization or nitriding of the jackets occurred. Embrittled fuel jackets occurred only when an alloy of U and SS was formed. Fuel received by ORNL is intact, no melting of jacket and slug has occurred and the NaK bond is free of uranium. It is unlikely, therefore, that U-SS steel alloy embrittlement is the cause of the present difficulties. The corroded outer appearance of the jackets following the steam cleaning operation makes nitriding a top suspect.

All of the uranium slugs recovered from the fuel rods exhibited from 10 to 30 mils camber and various degrees of pitting, probably depending upon their location in the reactor. Profilometer measurements made on a slug from a center rod of the cluster from the periphery of the reactor

---

[1] R. L. Ashley, R. J. Beeley, F. L. Fillmore, W. J. Hallett, B. R. Hayward, Jr., A. A. Jarrett, "SRE Fuel Element Damage Final Report," Atomics International, Canoga Park, California, NAA-SR-4488 (Suppl) June 30, 1961.

shows that the slug had swollen uniformly about 18 mils in diameter and exhibited very little pitting or discoloration, whereas, slugs from the reactor's center exhibited deep pits, eroded surface and various discolorations from gold, reddish brown, blue to a black color and were swollen irregularly up to 30 mils larger than the original 0.750-in.-OD slug.

The disposal of the liquid metal NaK collected under oil during processing progressed satisfactorily after enlarging the transfer lines which prevented the apparently heavily oxidized and waxy NaK from plugging the lines. A total of 29 batches of NaK (45 to 125 ml/batch) was transferred and reacted without incident or failure of a single component. Analysis of the NaK from three different clusters show the following concentrations:

	(1)	(2)	(3)
K (%)	-	78.56	79.89
Na (%)	-	21.44	20.11
O_2 (ppm)	-	5,450	4,700
Pu (c/m/g)	1.9×10^3	< 100	< 500
Cs^{137} (cpm/g)	2.3×10^6	3.0×10^7	2.5×10^7
U (ppm)	< 1.0	< 1.0	< 1.0
Gross β, (c/m/g)	9.56×10^5	1.7×10^7	1.02×10^7
Gross γ, thru pb, (c/m/g)	2.19×10^6	3.98×10^7	3.5×10^7

About 13 clusters of fuel remain to be processed, 10 clusters of which are being readied in carrier 2 for processing during the early part of August.

4.2 U-C Fuel Processing - B. A. Hannaford

Proposed reactor fuels of the uranium-graphite type contain particulate compounds (UO_2, UO_2-ThO_2, UC_2, UC_2-ThC_2) dispersed in a graphite matrix. Individual fuel particles, generally about 100 - 200μ in diameter, may be uncoated or coated with a refractory (Al_2O_3, pyrolytic carbon). The fuel element itself may be externally coated with SiC or associated with unfueled graphite.

Recovery of uranium and thorium from graphite fuels by a "semi-continuous" method appears to offer advantages over batch processing for fuels amenable to the nitric acid flowsheet: 90% HNO_3[1] and Grind-Leach.[2] Continuous flow of acid leach solution and wash water through a fixed bed of finely divided fuel should permit more efficient utilization of acid and wash water. To define a semi-continuous flowsheet, experimental data is needed on (1) the U and Th recovery as a function of contact time and flow rate of leach solution and wash water, and (2) permeability of deep beds of disintegrated fuel to acid and water.

Effect of Contact Time and Flow Rate on U Recovery. As a first step toward obtaining these data, two preliminary experiments were performed in which graphitized 3% U-graphite fuel cubes were disintegrated and leached in 90% HNO_3, at flow rates of ~6 gal $ft^{-2}hr^{-1}$ and ~12 gal $ft^{-2}hr^{-1}$.

Effluent samples, collected in ~100 ml increments, provided a measure of the rate at which uranium was removed from the dissolver. Figure 4.1 indicates that the run at the lower rate (and longer time) resulted in only

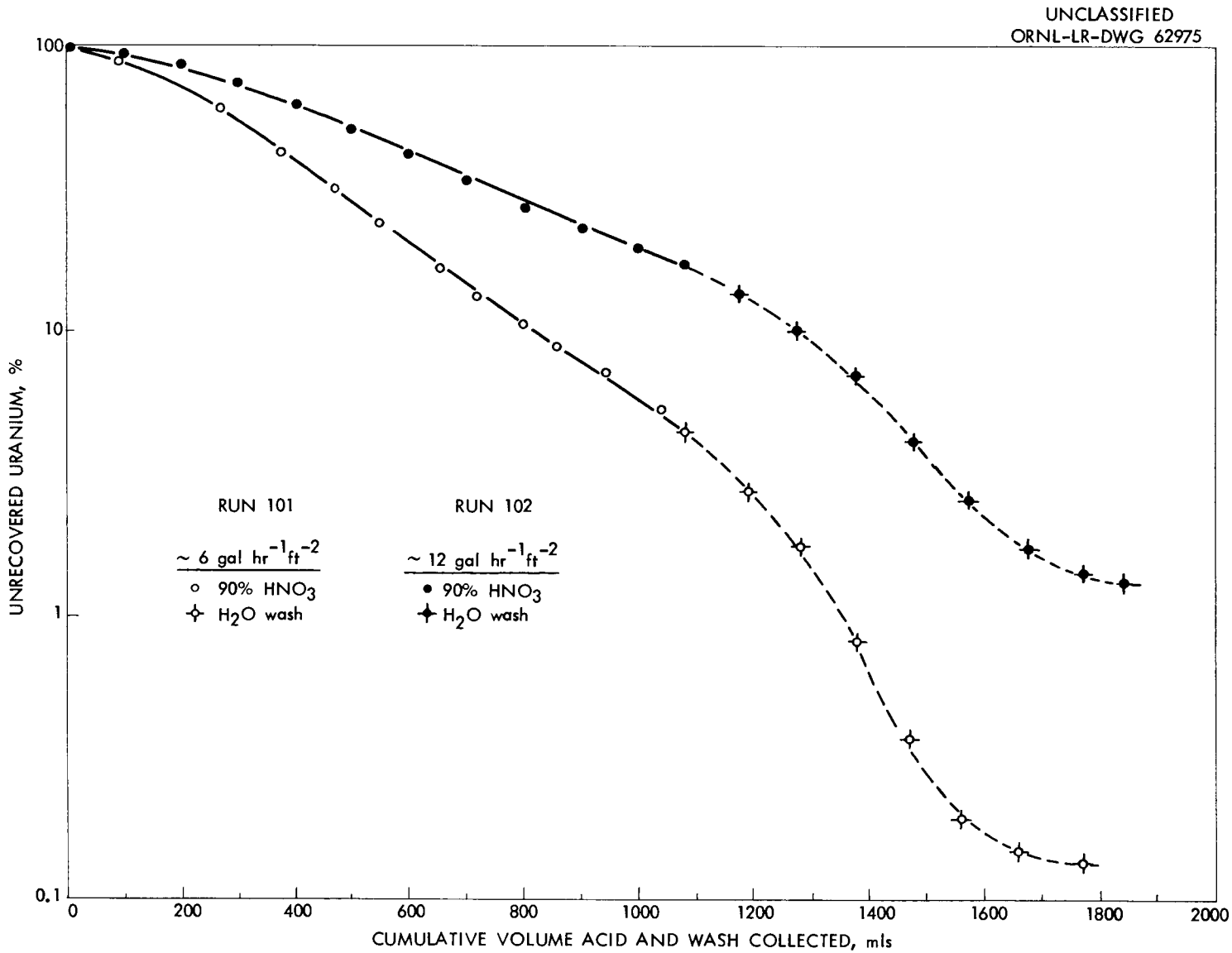

Fig. 4.1. Per cent uranium remaining in dissolver vs cumulative volume of acid and wash effluent, for 90% HNO_3 "Semi-Continuous" leaching of 3% U-graphite fuel. HNO_3/fuel = 3.35 l/kg. Temperature - 60°C.

0.13% U loss to the residue compared to a loss of 1.3% at the higher rate (and shorter time). Unfortunately, the experiment does not clearly show the relative importance of acid flow rate and total acid contact time. However, if the 90% HNO_3 curve for 12 gal $hr^{-1}ft^{-2}$ is extrapolated to 2000 ml acid, the U loss at this point is slightly less than for the 6 gal hr^{-1} ft^{-2} curve at 1000 ml, i.e., for the same total acid flow time. It appears that for these gross lumps of fuel some effect other than acid throughput rate is determining the uranium removal rate - even at these relatively low flow rates.

Comparison with results of successive batch leaching, summarized in Table 4.1, indicates the greater economy in acid volume and time for the continuous flow scheme, for essentially the same uranium recovery. Neither flowsheet has been optimized, therefore the comparison is only semi-quantitative.

Table 4.1. Comparison of Continuous vs Successive Batch Leaching:

3/8-in. Cubes of 3% U-Graphite Fuel in 90% HNO_3 at 60°C

	Continuous	Batch[3]
Acid/Fuel	3.35 liter/kg	4 leaches at 3.5 ℓ/kg = 14 ℓ/kg
Acid Contact Time	4.7 hr	4 leaches of 2 hr/each = 8 hr
Wash Water/Fuel	1.6 liter/kg	Not recorded
U loss to Residue	0.13%	0.099%

Permeability. Measurements of permeability of beds of disintegrated graphite fuel to acid and water are necessary for mechanical design of the processing equipment. Permeability may be defined as:

$$k = \frac{Qh_b \mu}{A\rho gh}$$

where

Q = total volume of liquid percolating in unit time

h_b = height of porous bed

μ = viscosity of liquid

A = plane area perpendicular to direction of flow

ρ = density of liquid

g = acceleration of gravity

h = pressure drop across bed, height of liquid

Employing the cgs system of units for the right-hand terms, the permeability constant, k, has units of cm^2.

Water permeability measurements made on the 2-in.-dia x 15-in. deep bed of thoroughly washed residue from run 102 indicated that the permeability "constant" was not constant, at least at the low pressure gradients which were employed. Apparent permeability was 3.2×10^{-6} cm^2 (at a pressure gradient of 0.5 cm H_2O/cm cake) or, expressed in engineering units, 142 gal/hr·ft^2 at 0.5 ft H_2O/ft. The significance of this high permeability is that the cubes of graphite fuel only partially disintegrated, due to the rigidity of the fixed bed. Such high permeability is no great advantage for a semi-continuous flowsheet and indicates that head end mechanical crushing of graphite fuel to, say 4 or 6 mesh might permit better solid-liquid contact with resulting higher leaching and washing rates - at the expense of lower permeability. Earlier measurements on identical fuel which had been mechanically degraded by a propellor agitator, after extended leaching, showed a permeability of ~25 gal/hr-ft^2 at 5.0 ft H_2O/ft. Permeability of the residue from pre-crushed material would likely not be lower than this.

Figure 4.2 is a schematic diagram of the experimental apparatus. An initial charge of 90% HNO_3 was heated to 60°C and maintained at temperature by hot water circulating through the dissolver jacket. The fuel charge, 430 g of 3/8-in. cubes, was poured into the dissolver and permitted to leach for 2-3 hours while intermittent agitation assisted in disintegration of the cubes and release of trapped off-gas. Metered addition of 90% HNO_3 was begun; continuous withdrawal of loaded solution through the supporting sand bed maintained a constant acid level in the dissolver. Following acid leaching, the drained bed was filled rapidly with water and continuous flow of water was maintained until after the color of the effluent indicated that it contained a negligible concentration of acid. The dissolver was drained, and the column of disintegrated graphite was discharged and sectioned for uranium analysis.

Efforts to reduce the swollen cubes of graphite fuel to a uniform bed of reasonably small particles were unsuccessful. In run 101, bursts of air were injected at the base of the dissolver; in run 102 a period of pulsing (30 cpm sinusoidal form, 0.25-in. amplitude) was followed by bursts of air. The principal effect was to round off the cubes. Visual examination of the washed residue showed that greater than 50% of the cubes were approximately their original size and shape. The residue was extremely friable and when dried and sieved, the mean particle size was 750μ for the top third of the bed, 1000μ for the bottom third.

References

1. L. M. Ferris, A. H. Kibbey, and M. J. Bradley, "Processes for Recovery of Uranium and Thorium from Graphite Fuel Elements. Part II," ORNL-3186 (in preparation).

2. M. J. Bradley and L. M. Ferris, "Recovery of Uranium and Thorium from Graphite Fuels. I. Laboratory Development of a Grind-Leach Process," ORNL-2761 (March 17, 1961).

3. Chemical Development Section B Monthly Report, April 1961.

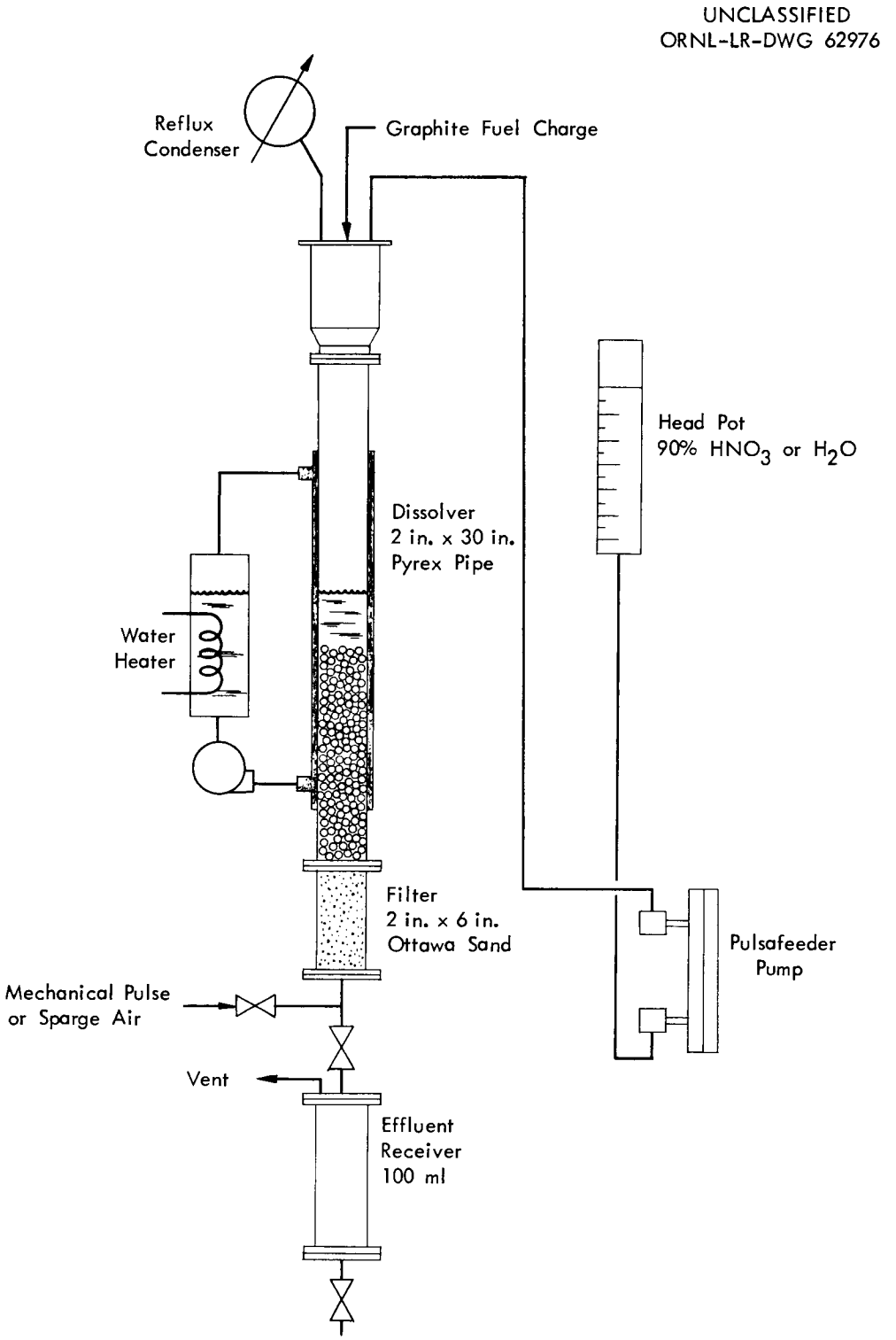

Fig. 4.2. Schematic diagram of experimental apparatus for semi-continuous leaching of U-graphite fuel.

5.0 SOLVENT EXTRACTION STUDIES

A. D. Ryon

5.1 Air Bubbler System for Control of Interface at the Bottom of a Pulse Column - A. N. Prasad, M. K. T. Nair, and F. L. Daley

The main purpose of the tests was to find out whether it is possible to use safely the air bubbler system for interface control in a pulse column operated with the interface at the bottom of the column. Two 2-in.-ID columns - 12 ft and 24 ft high - with nozzle plates of 23% and 10% free area, respectively, were tested. Tests for determining the flooding characteristics of the 12 ft column were also carried out.

The air bubbler system was essentially the same as that commonly used to detect the interface at the top of a column. Two air probes spaced vertically 20-in. apart were located at the bottom of the column. The differential pressure transmitter between the air probes was located above the top of the column to prevent backflow of liquid (Figure 5.1). The system was tested by circulating solvent and aqueous through the pulse column at a nominal flow rate of 1100 GSFH at 1-in. pulse amplitude and frequency of 50 cpm. The indicated interface position compared to actual level was determined at steady state and during ramp type interface transients.

Results with 12 ft Column. The control was satisfactorily demonstrated by an upward transient (Figure 5.2) in which an interface rise of 2-in./min was detected with less than 1-in. lag and a recovery time of only about 2 min. In a much more severe test made by a fast downward transient (12-in./min), the lag was 3 inches and the recovery time was about 5 minutes (Figure 5.3).

The main fault of the system was the loss of pulse in the air probes, nearly one half of the applied pulse amplitude of 1 inch was lost. Installation of snubbers in the air probes greatly reduced the loss of pulse, but caused spurious interface level indications when the air flow rate in either or both probes was varied.

The flooding rate for the column was determined by measuring the holdup of the aqueous phase in the column after operating at steady state for 1/2 to 1 hr at various throughputs. The throughput at which the holdup deviates from linearity was taken as the flooding point. Flooding rates for columns operated at 67 cpm (maximum attained with the pulser used) and a flow ratio of A:O = 1:2.7 with and without snubbers at 2/10 cfh air and no air (interface controlled manually in the latter case) are plotted in Fig. 5.4. The pulse amplitude in each case was 1-in. From a study of the effect of air purge rate on flooding for the above conditions, the holdup was found to decrease and the flooding rate increased with the air purge rate with no snubbers in the air purge lines. However, the flooding rate decreased when the snubbers were introduced into the air purge lines under the same operating conditions.

UNCLASSIFIED
ORNL-LR-DWG 62977

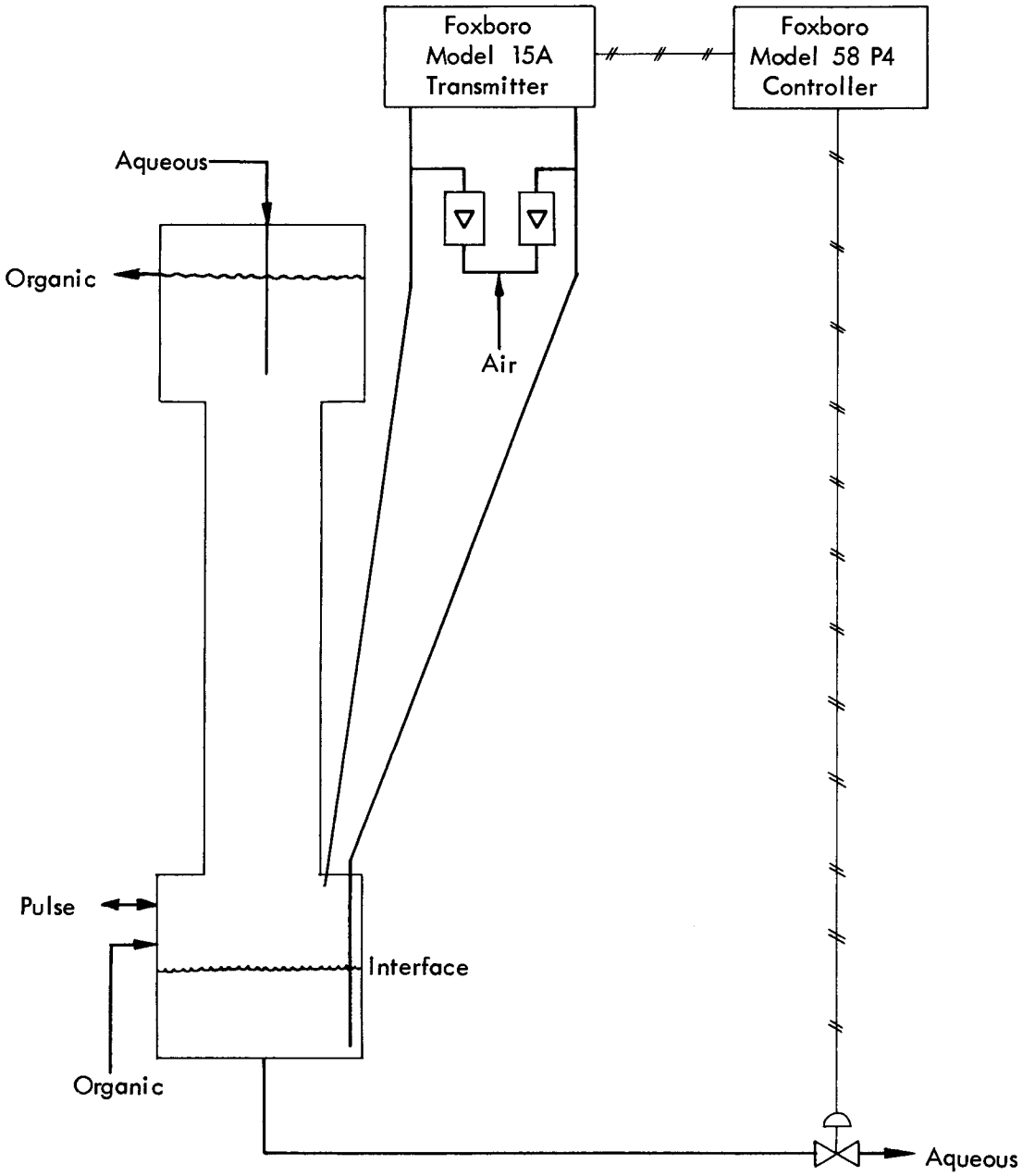

Fig. 5.1. Air bubbler system for bottom interface control.

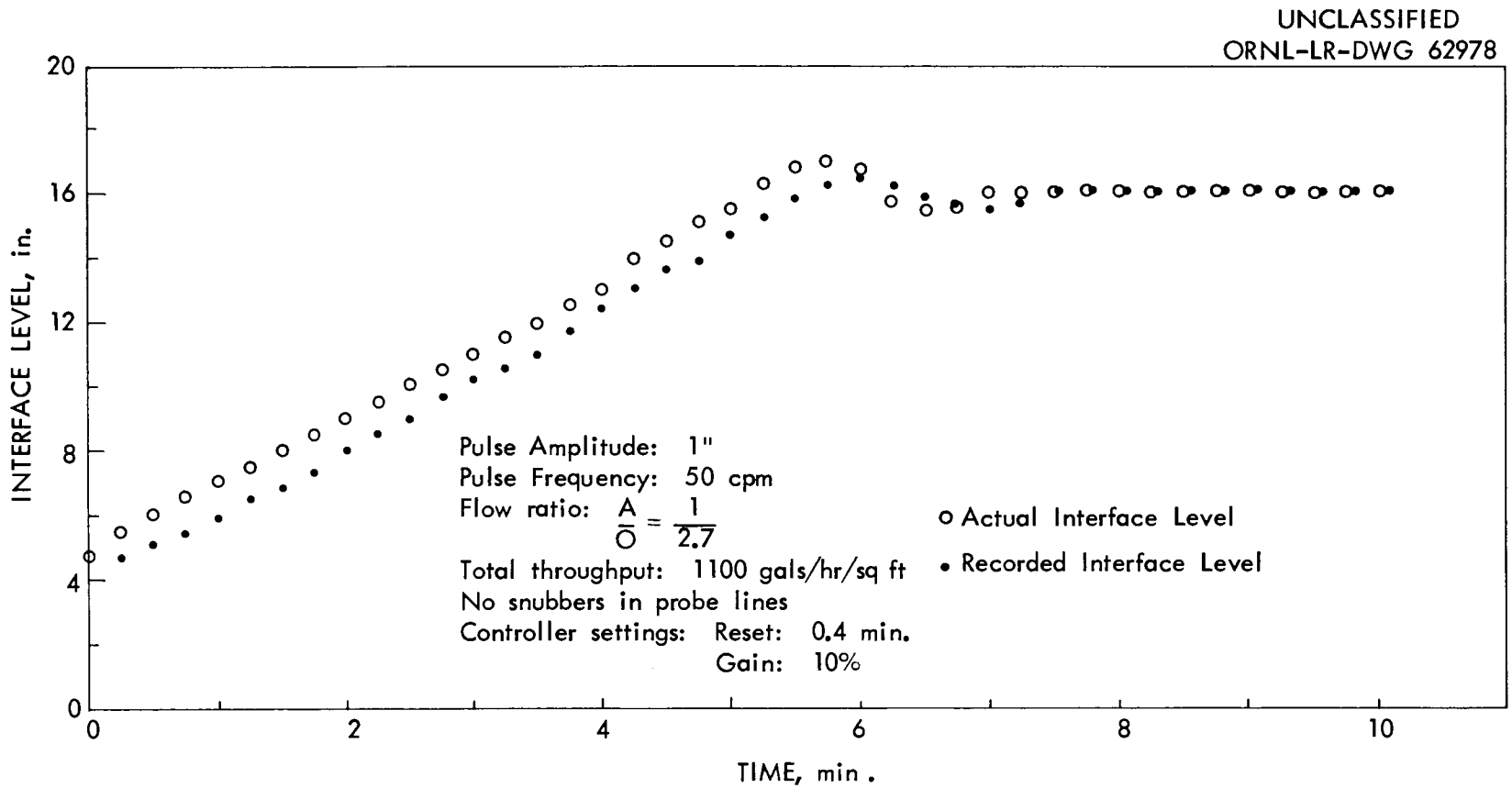

Fig. 5.2. Controller response curve for upward transient in 12 ft column.

UNCLASSIFIED
ORNL-LR-DWG 62979

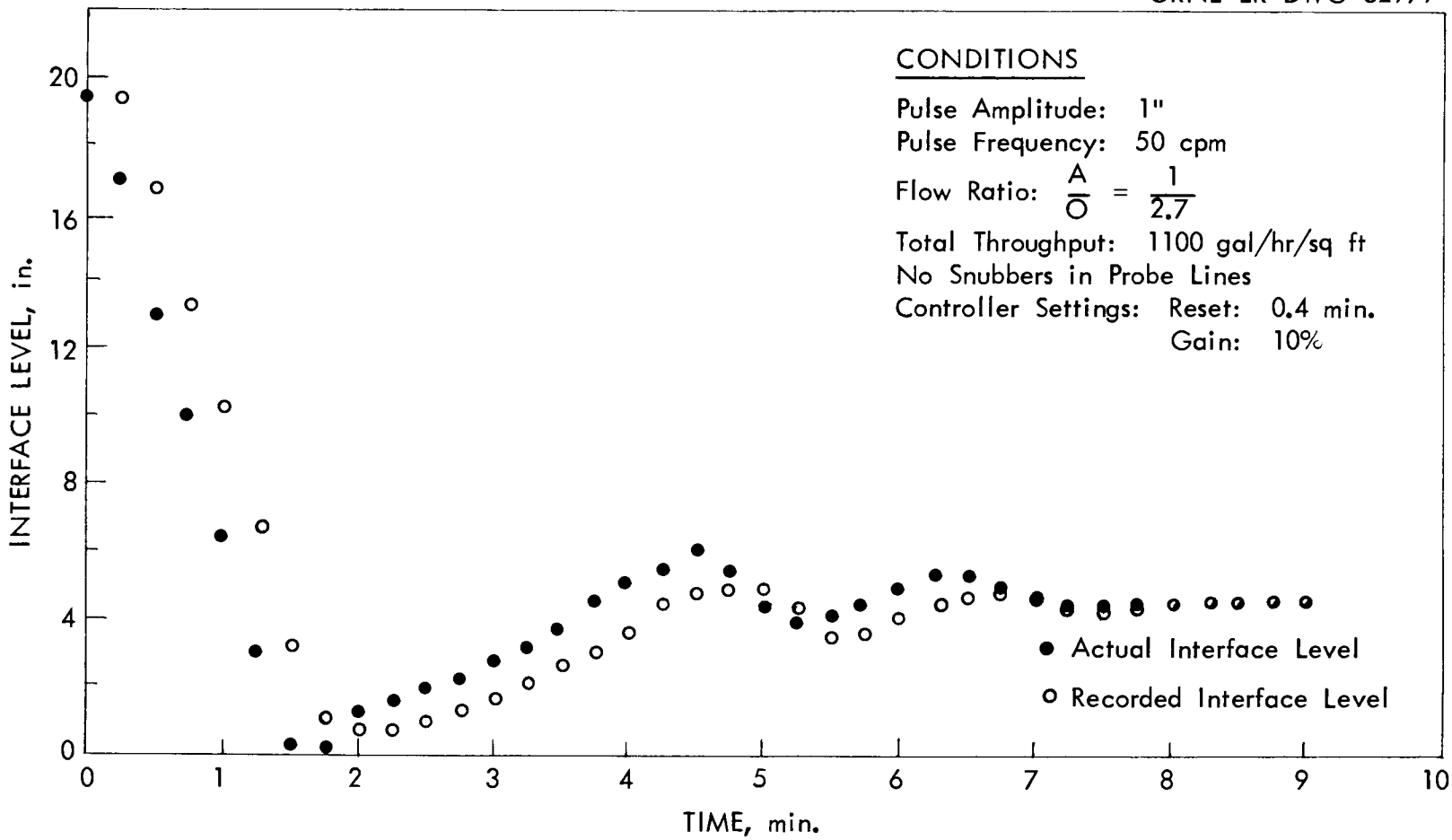

Fig. 5.3. Controller response curve for fast downward transient of interface in 12 ft column.

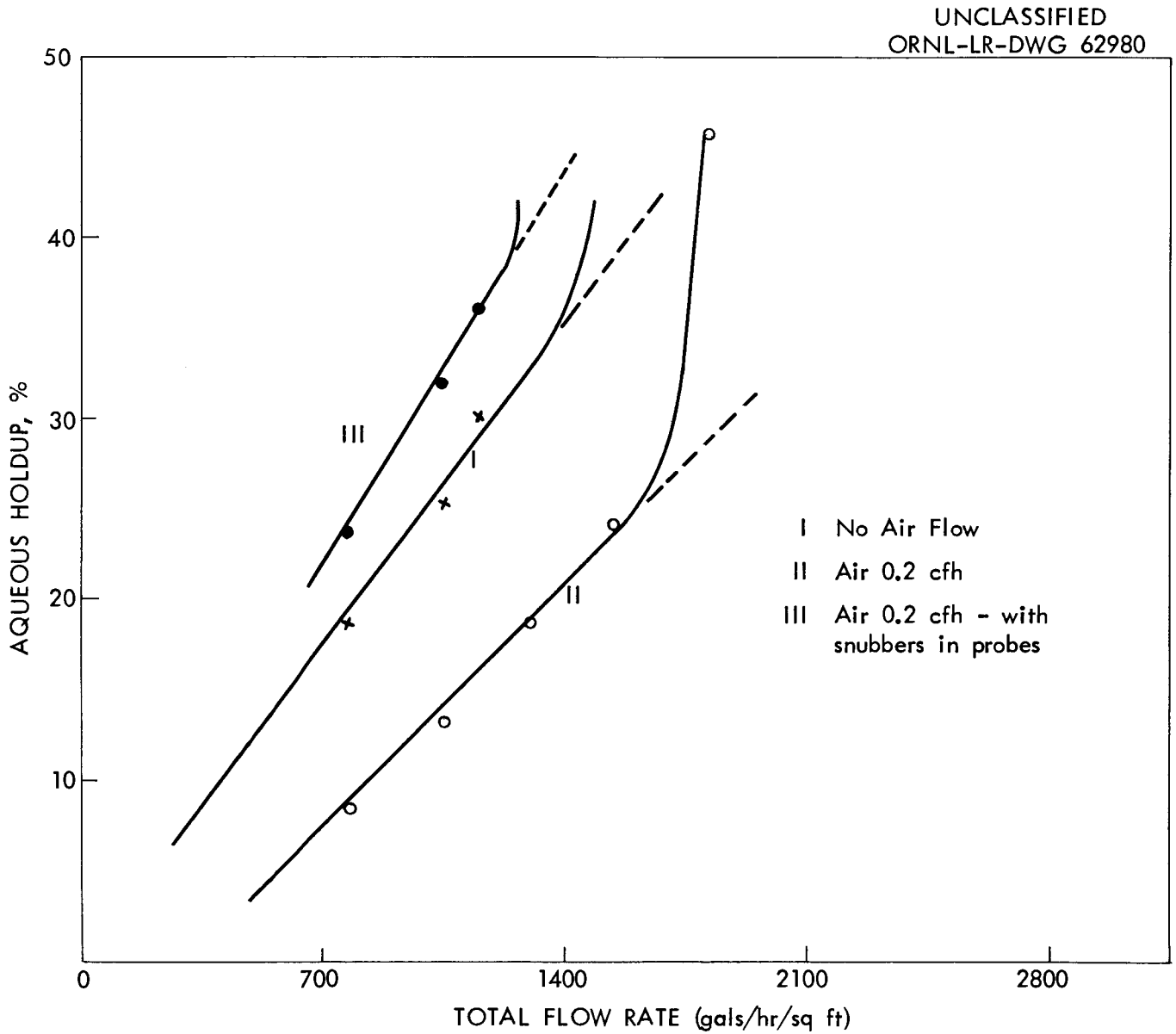

Fig. 5.4. Effect of air on holdup and flooding of 12 ft column.

Results with 24 ft Column. Attempts to control the interface were unsuccessful with either 1/8-in. or 1/4-in.-ID probes. Pulsations of the differential transmitter were approximately half the range of the instrument and obscured the response due to interface level. About 75% of the pulse was lost in the air probes and with 1/4-in.-ID probes the liquid penetrated nearly 2 ft in each probe on each pressure stroke of the pulser. The difference in viscosity and density of the organic phase in one probe and the aqueous phase in the other probably accounts for a slight loss of phasing and consequent large pulsation in the differential transmitter. This effect was much greater in the 24 ft column than in the 12 ft column because of the greater resistance to flow in the column due to its greater length and the use of nozzle plates with less free area.

6.0 TRANSURANIUM ELEMENT PROCESSING

P. A. Haas

Engineering studies are continuing for the chemical processing necessary for the transuranium element preparation program. The present emphasis is on the process equipment development and component testing necessary to the preliminary design of the processing facility. These include studies of disconnects, pumps, samplers, valves, and solvent extraction contactors.

6.1 Process Pump Development - T. S. Mackey

The transfer of process liquids and wastes will be done by steam jets or air actuated diaphragm pumps. A total of 33 sampling pumps will be required and a total of 10 process pumps. This does not include alternates for the replacement of the defective pumps.

Figure 6.1 represents a conceptual design for a pumping system using an air actuated diaphragm pump. The operation of the pump is as follows: (1) tanks T_1 and T_2 are maintained at approximately 30 psia and 5 psia, respectively, by an air pump P_1. The tanks will be connected by pipe lines to the diaphragm pump, (2) pumping action will be accomplished by switching the solenoid valves S_1 and S_2, (3) metered flow rates will be made possible by using an electrically timed switching arrangement that can be set for the desired time cycle. Various pipe line configurations may be used to actuate several pumps with a single vacuum pressure as shown in Figure 6.1.

Detailed drawings (C-34292, C-34293, C-34294) of a diaphragm pump which will deliver slightly in excess of 200 ml per minute at 35 strokes per minute with an outside diameter of 5-in. were prepared. The free deflection contour design was selected with dimensions which produce approximately 30,000 pounds per sq. in. maximum unit stress in the disphragm material. Theoretically an infinite life could be expected since the endurance limit of Hastalloy C is approximately 70,000 pounds per sq. in. However, this will not be the case since corrosive solutions carrying solid particles shorten the diaphragm life considerably.

The photographs show two sampling pumps mounted in the quick acting mounting rack (Figures 6.2 and 6.3). The ball check valves are made as a part of the quick inlet and outlet disconnect. Although this rack was made for only three pumps for test purposes the actual cubicle installation will be made large enough to accommodate 10 pumps in Cell 3, 10 pumps in Cell 4 and 13 pumps in Cell 5. The pressure gauge shown in the photograph was used to determine the value of the pressure and vacuum signal supplied to operate the diaphragm.

Test operation of the 2 pumps demonstrated that the pumps will successfully handle a saturated solution of lithium chloride through a suction lift of 13.5 ft. The maximum lift was found to be 23.5 in. of Hg for the first and 24 in. of Hg for the second pump. Diaphragm life tests will be performed when Hastalloy C is available.

UNCLASSIFIED
ORNL-LR-DWG 57133

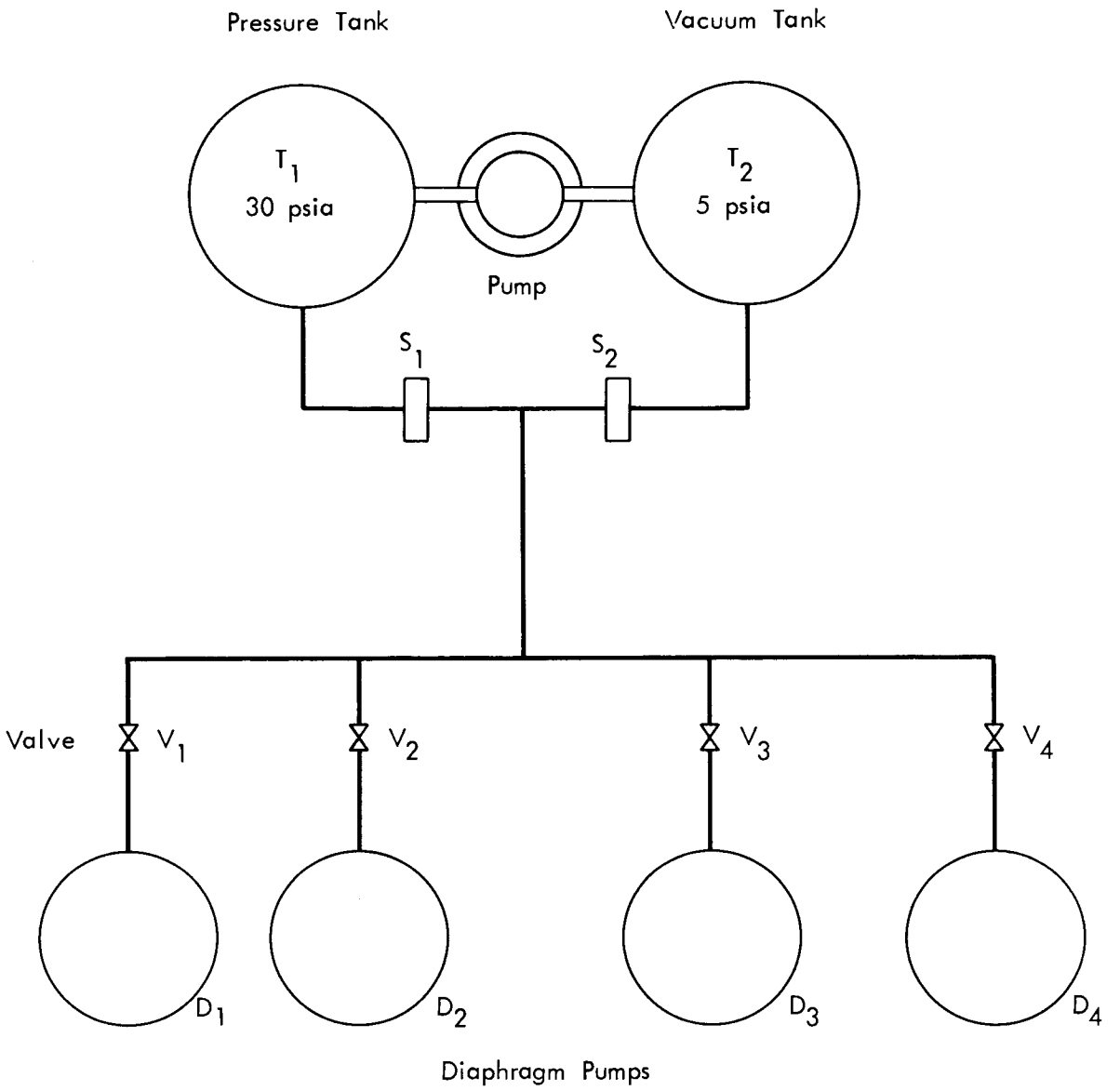

Fig. 6.1. Diaphragm pump actuation system.

UNCLASSIFIED
PHOTO 54423

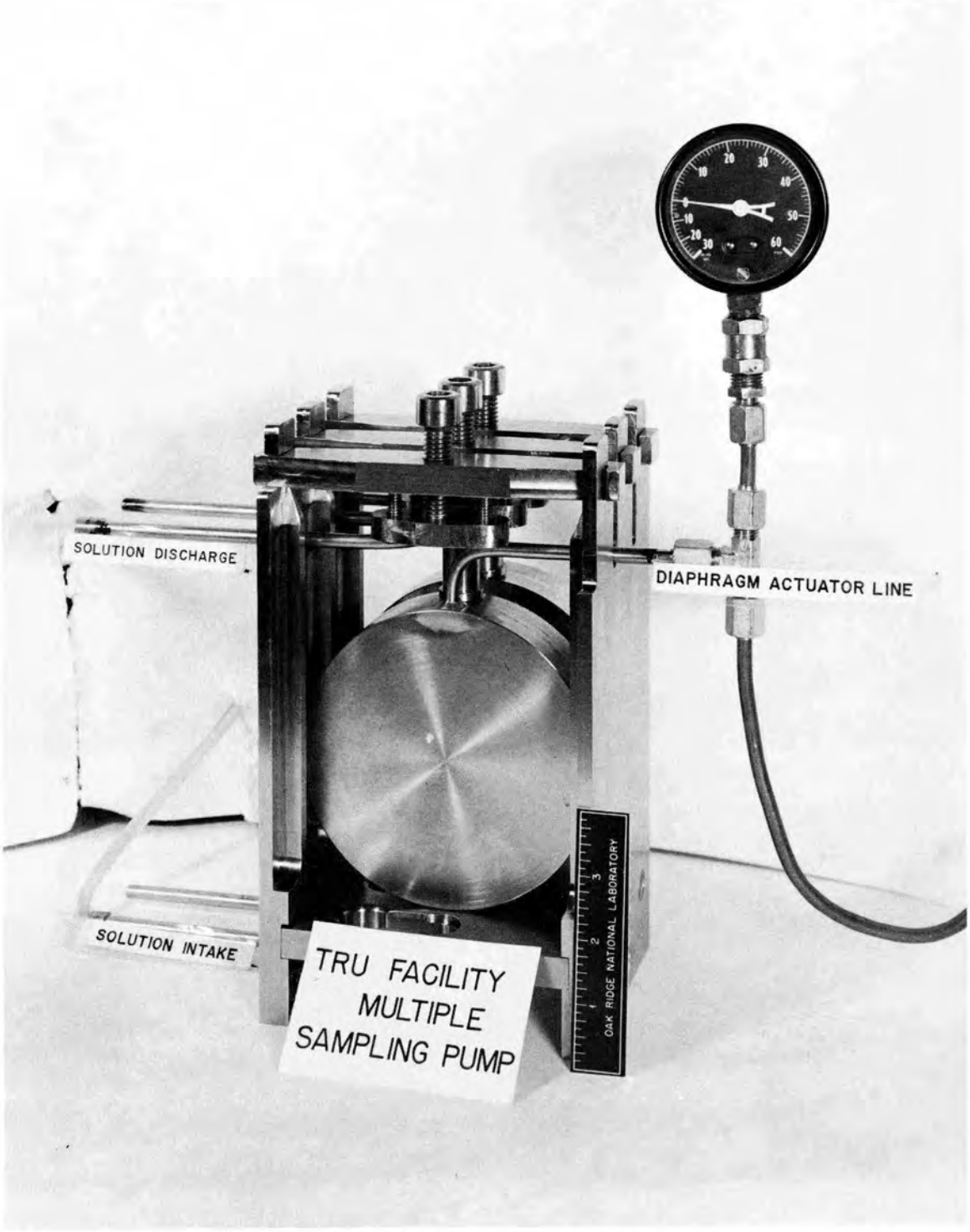

Fig. 6.2. Assembled view of TrU sampling pump and mounting rack.

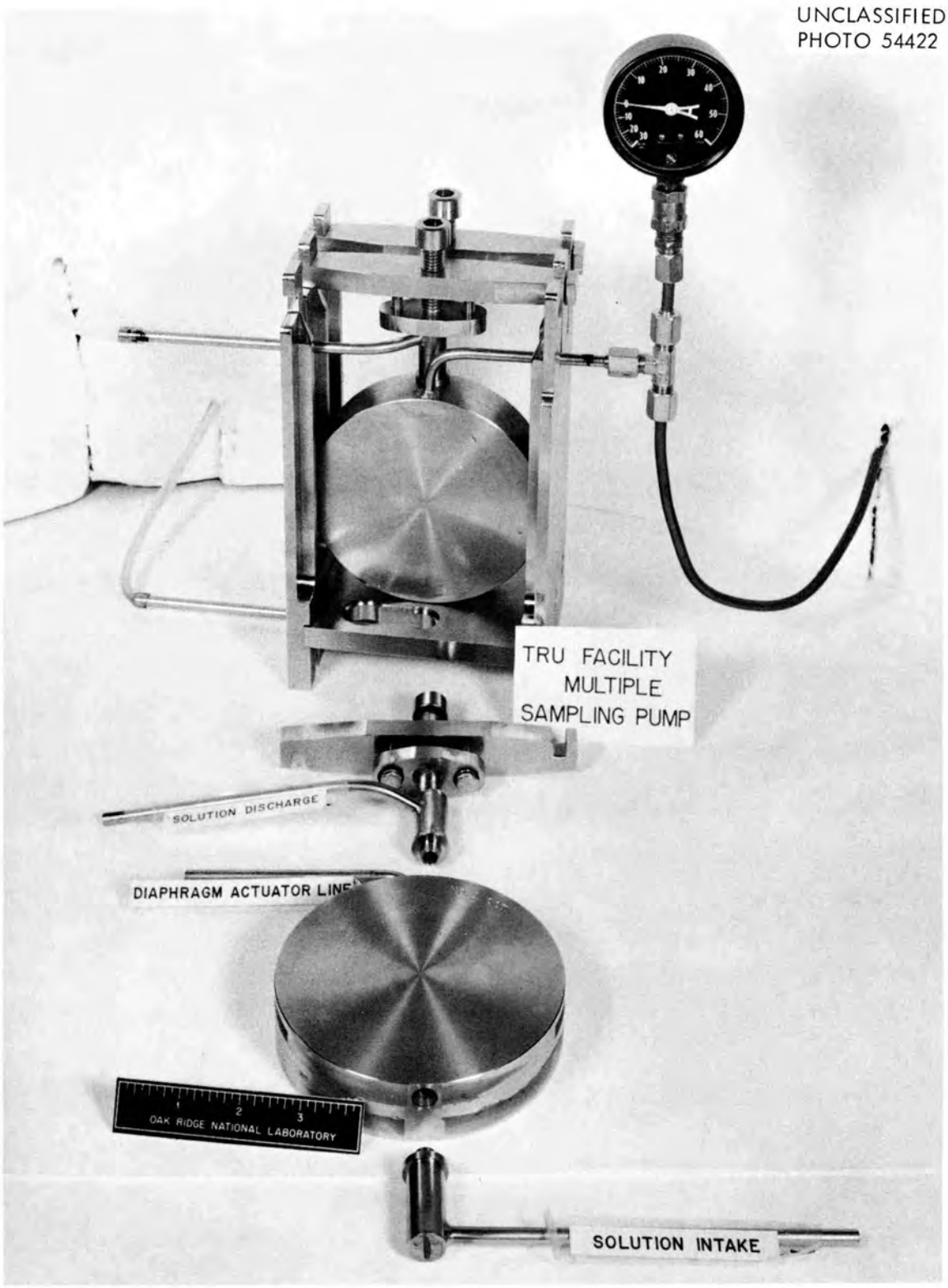

Fig. 6.3. Disassembled view of TrU sampling pump and mounting rack.

Although this type of pump requires the use of check valves it is thought that this disadvantage is outweighed by certain advantages such as metered flow rates, high suction lift, and the containment of process liquids in the actuating system in case of diaphragm rupture. The check valves will be replaceable as part of the connecting lines.

7.0 WASTE PROCESSING

J. C. Suddath

The purpose of this program is to obtain engineering information for the design of a hot pilot plant, which will demonstrate the disposal of high level waste solutions. Since the hot pilot plant may be built at the Idaho Chemical Processing site where TBP-25 waste is available, TBP-25 waste of the composition stored at Idaho was used for this test. This report covers the second TBP pot calcination test R-39.

7.1 Evaporator Calciner Test (R-39) - C. W. Hancher

Test R-39 was a repeat test of R-38 (Unit Operations Monthly Report, June 1961) using TBP-25 waste (Table 7.1). Nearly all of the operating conditions were the same for the two tests. Non-radioactive Ru was added to this test to determine its volatility during the evaporation-calcination operation. The average feed rate was 30.6 liters/hr. The recovery balances were: (Tables 7.2 and 7.3)

Nitrate	94.5%
Mercury	63.6%
Ruthenium	83.4%

The mercury concentrated in the evaporator during the standby operation as in test R-38.

7.2 Evaporator-Calciner Control and Operation

Test R-39 started with the evaporator filled with cold feed and the calciner empty and cold (Table 7.4). The evaporator contents are heated to boiling and then the calciner is heated and filled simultaneously requiring about 30 min to fill the calciner. As the control variables reached their set point conditions they were switched from manual to automatic control. The control settings for five controlled streams are shown in Tables 7.5, 7.6, and 7.7. The system controlled satisfactorily for over 90% of the time. The evaporator level controlled very well (Figure 7.1). It was within control limits at all times except when the level probe plugged and allowed the evaporator to fill to a high level.

The control of variables has been evaluated by the setting of limits:

Limit "A"	To high, out of control, dangerous
Limit "B"	Upper limit of good control
Limit "C"	Lower limit of good control
Limit "D"	Too low, out of control, uneconomical

The evaporator was out of the good control band twice. Above when the liquid level probe plugged and the steam shutdown due to a false signal. Below at the end of the test when the evaporator was on standby by an operator error.

The evaporator density control was good except when the evaporator was upset when the liquid level line plugged. The density was above the "B"

Table 7.1. Test R-39 Feed Concentration

	H^+ Molar	Al M	Hg g/ℓ	HNO_3 M	Fe g/ℓ	Na g/ℓ	Ru g/ℓ
As made up	1.26	1.72	4.0	6.6	0.16	2.4	
As analyzed							
Tank 1	1.70	1.76	4.00	7.02	0.214	-	0.113
Tank 2	1.71	1.75	3.95	7.04	0.217	-	0.173
Tank 3	1.69	1.77	3.98	7.08	0.242	-	0.151

Table 7.2. System Balances and Results, Test R-39

Nitrate Balance		
Input	3227 g moles	
Recovery		
(condensate	2823 g moles	87.48%
(solid	0.7 g moles	0.02%
(off-gas	40 g moles	1.20%
(evaporator	187.7 g moles	5.82%
		94.52%
Ruthenium Balance		
Input	0.685 g moles	
Recovery		
(condensate	-	-
(solid	0.529 g moles	77.23%
(evaporator	0.042 g moles	6.13%
		83.36%
Mercury Balance		
Input	9.29 g moles	
Recovery		
(condensate	1.77 g moles	19.05%
(solid	0.18 g moles	1.94%
(evaporator	3.96 g moles	42.63%
		63.62%

Off-gas

797 cu ft total
663 cu ft leakage and purge
134 cu ft non-condensable (102 cu ft oxygen)

134/489 = 0.274 cu ft/liter of system feed

Average Feed Rate

489/16 = 30.6 liter/hr average

Water Feed Rate

3630 liter of water, water to feed ratio = 7.4

Calcined Solids

33.2 kg, bulk density 0.56 g/cc

Table 7.3. Test R-39 Results

Test Time hrs	System Feed ℓ	System Water Feed ℓ	Water to Feed Ratio Ratio	System Condensate ℓ	Evap Press psig	Mol NO_3 Input g mol	Mol NO_3 Condensate g mol	Evap Density g/cc	Evap Temp °C	Evap Al Conc g/ℓ	Evap Hg Conc g/ℓ	Evap Ru Conc g/ℓ	Evap* H^+ Conc normality	Evap Steam Temp °C	Evap Steam Cond ℓ
1	107	26	0.24	82	-1.0	706	56	1.37	110.2	30.2	3.50	0.139	1.70	168	121
2	128	105	0.82	242	-1.0	845	230	1.26	110.7	46.8	5.59	0.486	3.62	124	301
3	188	184	0.98	384	-1.0	1241	507	1.35	117.2	33.1	3.96	0.258	3.48	124	505
4	225	332	1.48	551	-1.5	1485	637	1.27	111.6	50.4	6.53	0.213	2.64	137	661
5	267	438	1.64	715	-1.2	1762	945	1.35	118.3	48.6	6.25	0.176	1.90	123	895
6	304	510	1.68	893	-1.3	2006	1228	1.35	116.1	57.2	6.34	0.191	1.01	121	1129
7	334	650	1.95	1086	-1.2	2204	1467	1.35	116.8	65.6	8.90	0.239	0.36	135	1342
8	364	794	2.18	1269	-1.3	2402	1612	1.40	121.0	59.2	7.63	0.197	0.57	138	1563
9	380	991	2.61	1465	-1.5	2508	1741	1.36	118.1	57.2	7.75	0.177	0.62	145	1827
10	386	1195	3.10	1659	-1.3	2548	1890	1.32	111.4	37.8	4.26	0.097	0.61	144	2031
11	419	1252	2.99	1795	-1.0	2765	1921	1.25	110.9	84.1	8.08	0.201	2.07 AD	120	2211
12	442	1453	3.29	2012	-1.3	2917	1936	1.42	121.9	46.5	4.20	0.111	0.05 AD	120	2460
13	447	1726	3.86	2266	-1.3	2950	2246	1.27	118.7	85.4	10.00	0.236	0.54 AD	158	2790
14	484	1991	4.11	2559	-1.3	3194	2275	1.30	-	66.2	8.18	0.187	0.20 AD	157	3011
15	486	2173	4.47	2751	-1.3	3208	2336	1.36	120.0	67.3	9.90	0.194	0.10 AD	117	3266
16	489	2343	4.79	2984	-1.2	3227	2401	1.40	119.8	66.2	11.50	0.193	0.20 AD	146	3515
17		2483	5.08	3162	-1.2		2446	1.37	120.8	64.8	13.5	0.177	0.20 AD	146	3779
18		2672	5.46	3352	-1.2		2492	1.36	120.4	64.4	14.0	0.208	0.20 AD	147	4043
19		2846	5.82	3538	-1.2		2533	1.36	120.0	63.7	18.3	0.220	0.28 AD	146	4298
20		3035	6.21	3725	-1.2		2563	1.36	119.6	63.0	10.5	0.185	0.02 AD	145	4553
21		3232	6.61	3920	-1.2		2596	1.36	118.7	61.9	23.7	0.208	0.02 AD	144	4802
22		3399	6.95	4117	-1.1		2628	1.37	118.7	60.0	28.0	0.183	0.16 AD	144	5051
23		3562	7.28	4308	-1.2		2651	1.36	117.0	66.5	30.9	0.169	0.32	142	5180
24		3630	7.42	4407	-1.2		2664	1.36	110.0	56.6	28.3	0.160	0.88	133	5212
25		3630	7.42	4457	-1.2		2672	1.32	106.2	49.3	26.0	0.150	1.32	115	5244
26		3630	7.42	4549	-1.2		2722	1.30	105.0	56.1	36.2	0.163	1.73	112	5276
27		3630	7.42	4594	-1.2		2749	1.35	108.6	61.1	43.3	0.185	2.00	113	5319
28		3630	7.42	4648	-1.2		2779	1.37	107.9	56.1	34.0	0.185	2.04	116	5356
29		3630	7.42	4735	-1.2		2823	1.37						118	5392
30		3630	7.42											117	

* AD (Acid Defficiency)

Table 7.3. (Continued)

Test Time	Calciner Heat Input	Calciner Temp at Feed Point	Calciner Temp at Mid-Section Center	System Off-gas	Off-gas before Water Scrub					Vol Air	Off-gas after Water Scrub				
					N_2 78.03	O_2 21.00	Ar 0.94	$N_2O + CO_2$ 0.03	NO_2		N_2	O_2	Ar	$N_2O + CO_2$	NO_2
hrs	KWH	°C	°C	cu ft	vol %	vol %	vol %	vol %	vol %	cu ft	vol %	vol %	vol %	vol %	vol %
1	48	120	120	180	77.4	20.9	0.9	0.1	0.1	10.9	77.9	20.9	0.9	0.2	-
2	94	135	135	18	77.1	20.6	0.9	0.8	0.2	17.8	77.6	20.7	0.9	0.3	-
3	135	140	140	37	77.3	20.5	0.9	1.0	< 0.1	18.8	78.1	20.7	0.9	0.3	-
4	183	140	140	55	69.4	27.9	0.8	1.0	0.1	16.0	74.0	24.2	0.9	0.4	-
5	228	140	140	75	61.7	35.8	0.7	1.2	0.2	15.8	61.4	37.1	0.8	0.5	-
6	264	135	135	100	68.1	30.2	0.8	0.5	0.2	21.8	56.1	42.9	0.7	0.6	-
7	290	130	130	126	51.5	46.4	0.7	1.4	0.5	17.2	55.0	43.3	0.7	0.6	-
8	311	135	135	153	50.3	47.5	0.6	1.3	0.8	17.4	52.9	45.8	0.7	0.7	-
9	329	135	135	179	54.2	43.5	0.6	1.1	0.7	18.1	61.2	37.1	0.7	0.6	-
10	351	135	135	204	77.9	21.0	0.9	-	0.1	25.0	59.0	39.6	0.7	0.6	-
11	367	130	130	239	62.6	34.4	0.7	0.9	1.1	28.1	61.0	38.5	0.7	0.2	-
12	383	130	130	256	67.1	30.5	0.8	0.7	0.8	14.6	68.1	30.8	0.8	0.2	0.2
13	399	130	130	282	65.3	32.1	0.8	1.0	1.3	21.8	61.2	36.9	0.7	0.7	0.4
14	414	130	130	312	62.0	35.9	0.7	0.9	0.7	23.9	63.3	35.7	0.8	0.2	0.2
15	426	135	135	339	62.2	36.0	0.7	1.1	0.4	21.5	63.7	34.9	0.8	0.5	0.1
16	432	160	135	369	62.3	35.7	0.7	1.0	0.7	24.0	63.1	35.7	0.8	0.5	0.2
17	449	240	125	398	61.0	36.6	0.7	1.1	0.9	22.7	63.1	35.8	0.8	0.4	0.2
18	456	270	135	428	62.1	35.8	0.7	1.0	0.8	23.9	63.8	35.4	0.8	0.2	0.1
19	468	360	140	458	61.3	36.1	0.7	1.5	0.6	23.6	63.1	35.7	0.8	0.2	0.2
20	482	440	140	488	61.2	36.8	0.7	0.9	0.6	23.6	64.0	35.3	0.8	0.3	0.2
21	494	560	150	518	63.1	34.5	0.7	1.1	0.6	24.3	63.5	35.1	0.8	0.5	0.2
22	504	635	150	547	64.8	32.7	0.7	1.1	0.7	24.1	67.0	32.0	0.8	0.4	0.2
23	510	735	160	580	68.6	29.3	0.7	1.0	0.7	29.0	69.6	28.4	0.7	1.0	0.2
24	521	750	165	619	74.7	23.7	0.7	0.2	0.6	37.4	75.8	22.9	0.7	0.3	0.1
25	530	760	180	641	-	-	-	-	-	-	75.5	23.2	0.7	0.3	0.2
26	538	760	210	686	75.8	22.4	0.7	0.1	0.7	43.7	75.6	22.9	0.7	0.2	0.2
27	547	760	260	711	75.9	22.3	0.7	0.2	0.7	24.3	76.2	22.3	0.7	0.3	0.2
28	557	770	370	748	77.1	21.4	0.7	0.1	0.8	36.6	77.2	21.3	0.7	0.3	0.2
29	566	775	485	786	77.1	21.0	0.7	0.1	0.8	37.5	77.6	21.1	0.8	0.1	0.2
30					77.2	21.2	0.7	0.2	0.4	-	77.3	21.6	0.7	0.1	0.1
31					77.9	20.9	0.9	< 0.1	< 0.1		78.0	21.1	0.9	< 0.1	< 0.1

Table 7.4. Test R-39 Log

Time	
9:00 am	Pot feed started - Wheelco 800°C set point
9:30 am	Pot full
10:00 am	Water to evaporator on manual most of test
5:40 pm	Wheelco set point changed from 800 to 850°C
7:40 pm	Pot and evaporator liquid level probes plugged
10:00 pm	Evaporator control temperature burn out - switch to alternate
11:00 pm	Feed valve open but no flow (valve ok, line plugged in pot)
12:00 am	Feed off, evaporator on standby
2:00 am	Calciner off, all temperatures above 485°C

Table 7.5. Control Ranges for Test R-39

	Control Variable	Control Range 0 - 100%	Prop Band %	Reset min	Set Point[a] Scale, %
Evaporator	Liquid level	7.4-55.0 liter	250	5	50
Evaporator	Density	1.0-1.5 g/cc	200	10	70
Evaporator	Temperature	101-128°C	100	5	65
Evaporator	Pressure	-5 to +5 psig	10	0.3	42
Calciner	Liquid level	44-52 liter	100	10	50

[a]See Table 7.7.

Table 7.6. Operational Limits for Test R-39

	Limit A	Limit B	Set Point	Limit C	Limit C	Operational Readings* Min	Max
Evaporator Liquid level							
scale %	50	65	50	55	25	28	68
liters	33	26	22	18	15	16	27
Evaporator Density							
scale %	80	80	70***	50	40	53	85
g/cc	1.40	1.35	1.32	1.25	1.20	1.26	1.42
Evaporator Temperature							
scale %	90	75	65	30	0	37	85
°C	122	120	117	110	103	111	121
Evaporator Pressure							
scale %	47	45	42	40	38	45	35
psig	-0.25	-0.50	-0.75	-1.0	-1.25	-0.5	-1.5
Calciner Liquid level							
scale %	30	40	50	60	70	20	100**
liters	58	59	60	61	62	57	68

* Recorded hourly readings
** Was zero before and after filling period
*** Al $\cong$ 45 g/liter

Table 7.7. Control Settings for Test R-39

Time	Evaporator Density			Evaporator Liquid Level			Evaporator Temperature			Evaporator Pressure			Pot Liquid Level		
	Set Point	Prop Band	Reset	Set Point	Prop Band	Reset	Set Point	Prop Band	Reset	Set Point	Prop Band	Reset	Set Point	Prop Band	Reset
	%	%	min	%	%	min	%	%	min	%	%	min	%	%	min
0900	70	200	10	50	150	5	65	100	2	45	25	0.3	50	400	5
1000	70	200	10	50	150	5	70-M*	-	-	45	25	0.3	50	400	5
1100	70	200	10	50	200	5	65-M	-	-	45	25	0.3	50	400	5
1200	70	200	10	50	200	5	65	100	2	45	25	0.3	50	400	5
1300	70	200	10	50	200	5	65	100	2	45	25	0.3	50	400	5
1400	70	200	10	50	200	5	65	100	2	45	25	0.3	50	100	5
1500	70	200	10	51	100	5	57-M	-	-	43	25	0.3	50	100	5
1600	70	200	10	50	100	5	57-M	-	-	43	25	0.3	50	100	3
1700	70	200	10	50	100	5	60-M	-	-	43	25	0.3	50	100	5
1800	70	200	10	50	100	5	65-M	-	-	43	25	0.3	50	50	3
1900	70	200	10	50	100	5	70-M	-	-	43	25	0.3	50	50	3
2000	70	200	10	60	100	5	75-M	-	-	43	25	0.3	50	50	3
2100	70	200	10	70	100	5	80	100	2	43	25	0.3	50	50	3
2200	70	200	10	50	100	5	75	100	2	43	25	0.3	50	50	3
2300	70	200	10	50	100	5	65	100	2	43	25	0.3	50	50	3
2400	70	200	10	50	100	5	65	100	2	43	25	0.3	50	50	3

* Manual Operation

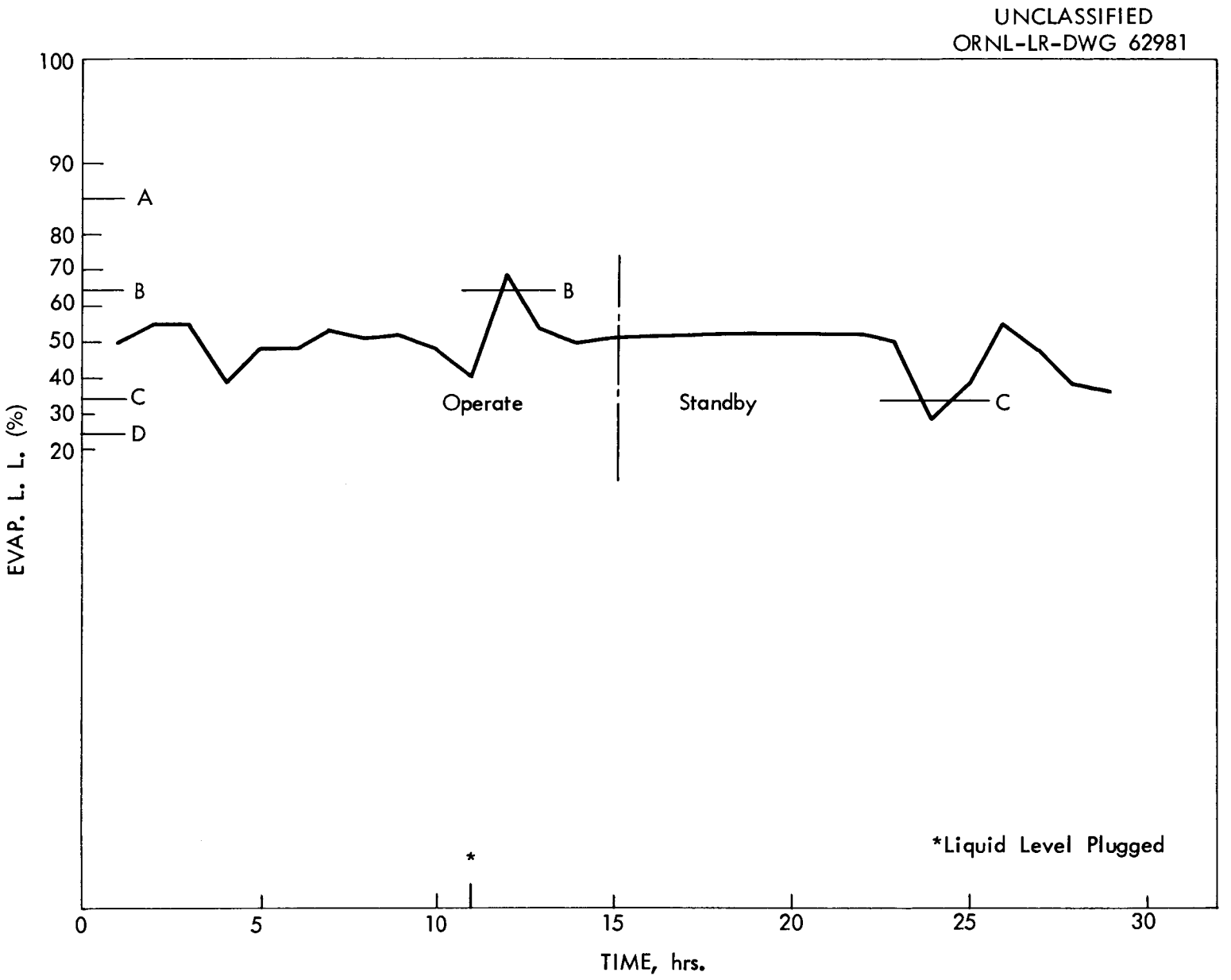

Fig. 7.1. Test - R-39 - Evap. Liquid Level.

limit only once (Figure 7.2). The evaporator temperature which was hoped to be a function of the evaporator acid concentration with a set of 117°C only exceeded the "B" limit (120°C) twice, once while the evaporator liquid level upset, and once before (Figure 7.3). The 117°C set point was picked up to produce an acid concentration in the evaporator of 5 to 6 M. However, the acid in the evaporator was much lower averaging about one molar. Much less water could have been added to remove the acid, if a higher temperature set point had been picked (Figure 7.4). The water to feed ratio was 7.4. If a 3 to 1 ratio had been used at a temperature of about 120°C, the operation would be nearer ideal.

The calciner liquid level control fluctuated too greatly at 400% proportional band so the band width was reduced to 100%, Table 7.7. However, this did not stop the cycling. The calciner cycling caused cycling in the evaporator. In test R-39 the pump pressure to the calciner feed valve fell to about 1 to 2 psig. This reduced the valve capacity, but also allowed the valve to remain partially open all of the time.

7.3 Calciner Pot Corrosion

The calciner pot used in test R-39 showed no signs of corrosion on the inside. The outside of the pot showed no signs of corrosion or oxidation scaling. A nitrogen purge of 10 cu ft/hr was used between the calciner pot and furnace liner.

7.4 Calcined Solid

The calcined solid had a bulk density of 0.56 g/cc (Tables 7.2 and 7.8). The solid was light gray in color and very crumbly. There was a hole down the center of the pot indicating radial growth of solids. Only 2% of the mercury fed to the system remained with the calcined solids. However, 77% of the ruthenium added as cold ruthenium remained with the calcined solid. The off-gas line contained a solid film which was 90% mercury and 1% Ru. The mercury and ruthenium system balances were 63% and 83%. The unaccounted for material probably plated on the system's metal surfaces.

Table 7.8. R-39 Solid Analysis

	Al wt %	Hg wt %	HNO_3 wt %	Ru wt %
Top	50.6	0.007	< 0.1	0.17
Middle	45.5	0.32	0.38	0.17
Bottom	50.4	0.007	< 0.1	0.15

UNCLASSIFIED
ORNL-LR-DWG 62982

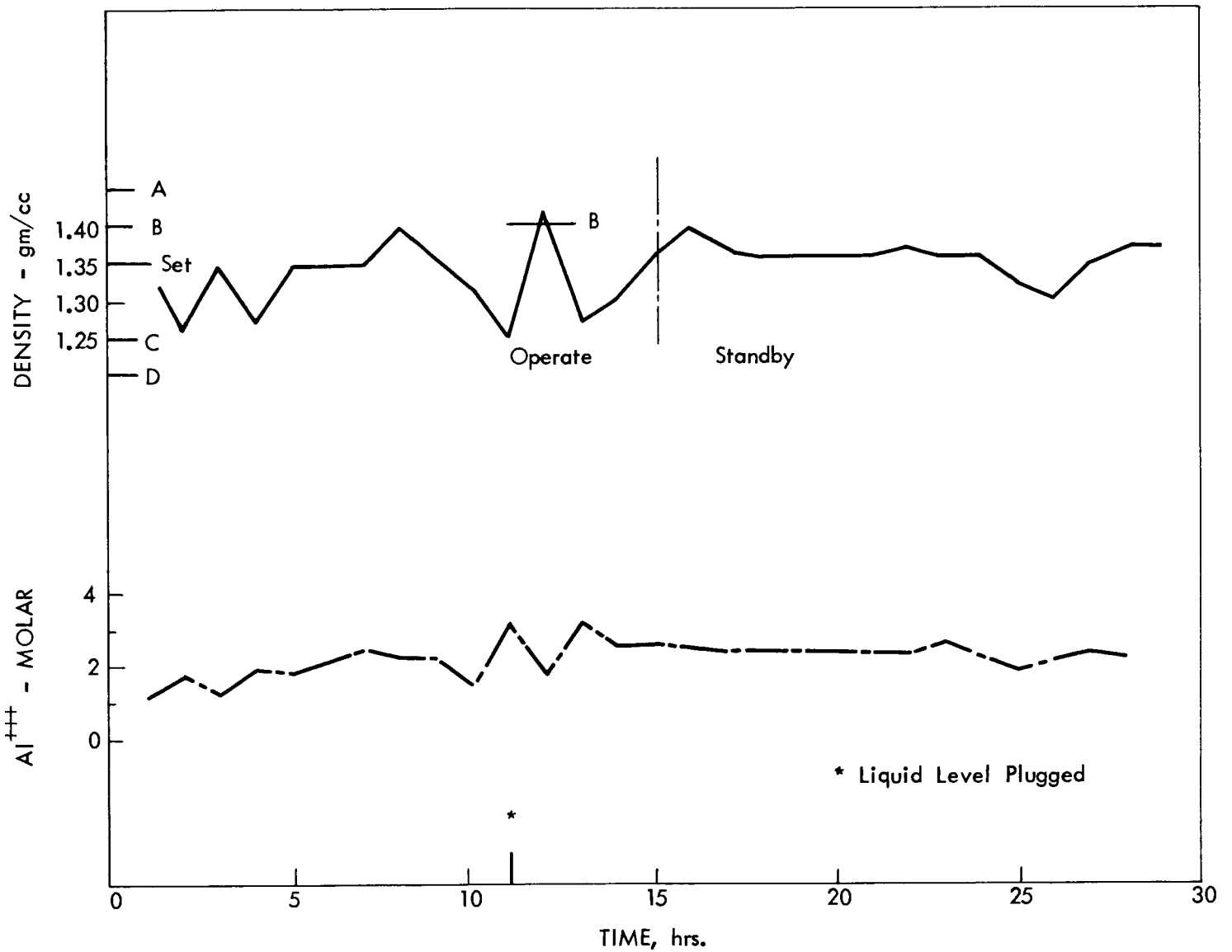

Fig. 7.2. Test - R-39 - Evap. density and Al^{+++} concentration.

UNCLASSIFIED
ORNL-LR-DWG 62983

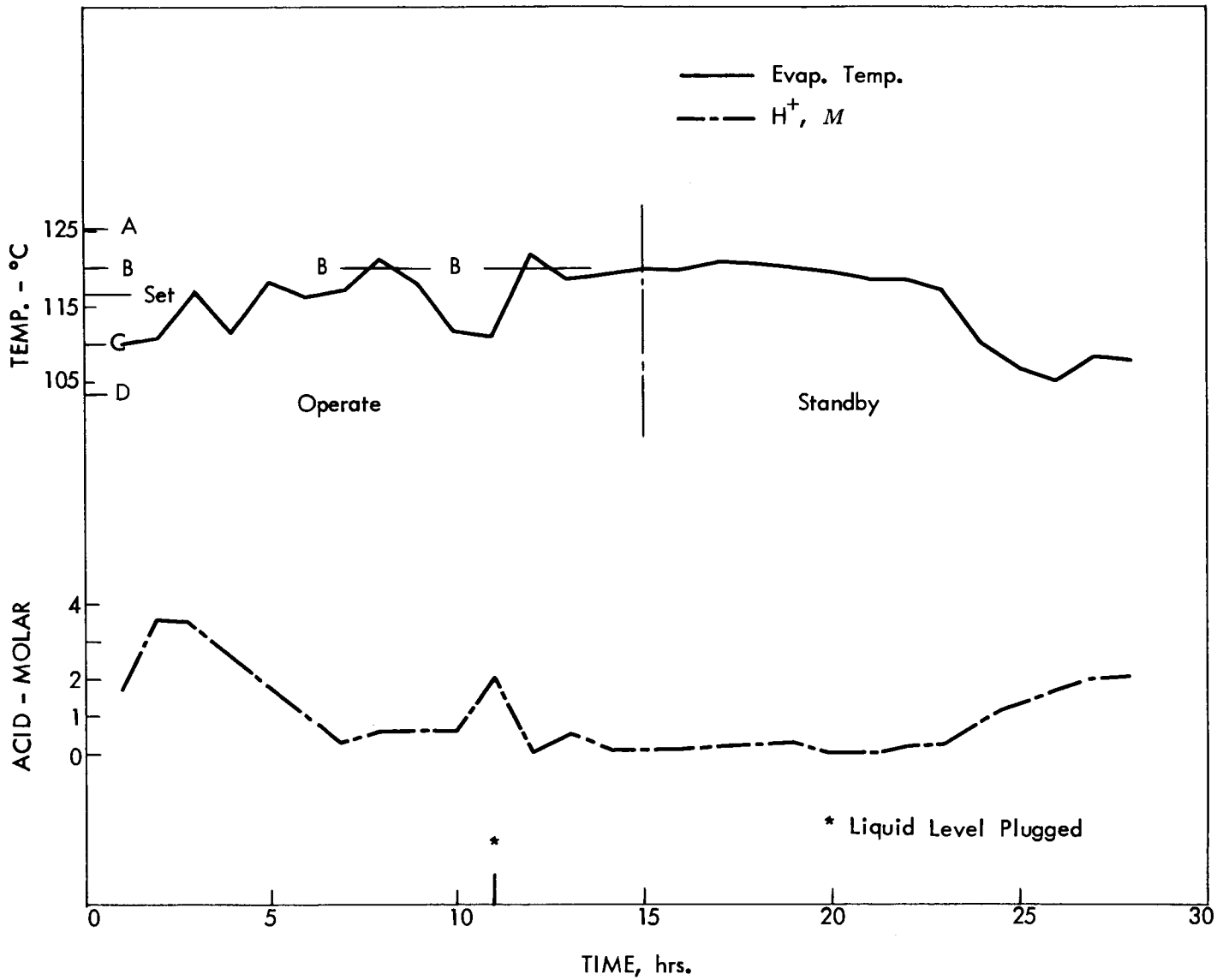

Fig. 7.3. Test - R-39 - Evap. Acid and temperature.

UNCLASSIFIED
ORNL-LR-DWG 62984

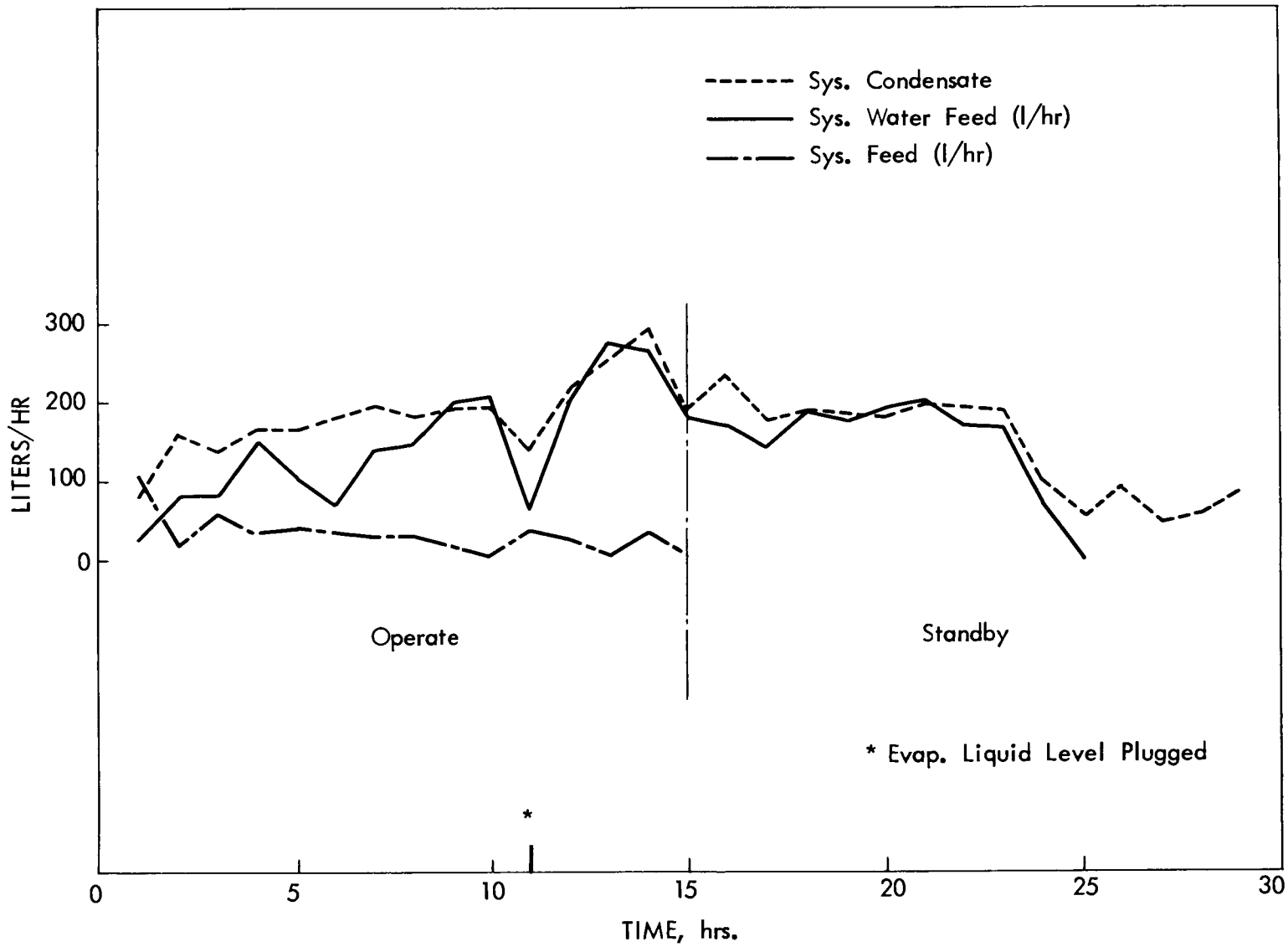

Fig. 7.4. Test - R-39 - Flow conditions.

DISTRIBUTION

1. E. L. Anderson (AEC Washington)
2. F. P. Baranowski (AEC Washington)
3. W. G. Belter (AEC Washington)
4. S. Bernstein (Paducah)
5. R. E. Blanco
6. J. O. Blomeke
7-10. J. C. Bresee
11. R. E. Brooksbank
12. K. B. Brown
13. F. R. Bruce
14. J. A. Buckham (ICPP)
15. L. P. Bupp (HAPO)
16. W. D. Burch
17. W. H. Carr
18. G. I. Cathers
19. J. T. Christy (HOO)
20. W. E. Clark
21. V. R. Cooper (HAPO)
22. K. E. Cowser
23. F. E. Croxton (Goodyear Atomic)
24. F. L. Culler, Jr.
25. W. Davis, Jr.
26. O. C. Dean
27. D. E. Ferguson
28. L. M. Ferris
29. R. J. Flanary
30. E. R. Gilliland (MIT)
31. H. E. Goeller
32. M. J. Googin (Y-12)
33. H. B. Graham
34. A. T. Gresky
35. P. A. Haas
36. M. J. Harmon (HAPO)
37. F. E. Harrington
38. L. P. Hatch (BNL)
39. O. F. Hill (HAPO)
40. J. M. Holmes
41. R. W. Horton
42. A. R. Irvine
43. G. Jasny (Y-12)
44. H. F. Johnson
45. W. H. Jordan
46. S. H. Jury
47. K. K. Kennedy (IDO)
48. B. B. Klima
49. E. Lamb
50. D. M. Lang
51. S. Lawroski (ANL)
52. R. E. Leuze
53. W. H. Lewis
54. J. A. Lieberman (AEC Washington)
55. R. B. Lindauer
56. A. P. Litman
57. J. T. Long
58. B. Manowitz (BNL)
59. J. L. Matherne
60. J. A. McBride (ICPP)
61. J. P. McBride
62. W. T. McDuffee
63. R. A. McGuire (ICPP)
64. R. A. McNees
65. R. P. Milford
66. J. W. Morris (SRP)
67. E. L. Nicholson
68. J. R. Parrott
69. F. S. Patton, Jr. (Y-12)
70. H. Pearlman (AI)
71. R. H. Rainey
72. J. T. Roberts
73. K. L. Rohde (ICPP)
74. C. A. Rohrmann (HAPO)
75. A. D. Ryon
76. W. F. Schaffer, Jr.
77-79. E. M. Shank
80. M. J. Skinner
81. C. M. Slanksy (ICPP)
82. S. H. Smiley (ORGDP)
83. J. I. Stevens (ICPP)
84. C. E. Stevenson (ANL, Idaho)
85. K. G. Steyer (General Atomics)
86. E. G. Struxness
87. J. C. Suddath
88. J. A. Swartout
89. F. M. Tench (Y-12)
90. V. R. Thayer (duPont, Wilmington)
91. W. E. Unger
92. J. Vanderryn (AEC ORO)
93. F. M. Warzel (ICPP)
94. C. D. Watson
95-124. M. E. Whatley
125. G. C. Williams
126. R. H. Winget
127. C. E. Winters
128. R. G. Wymer
129-130. Central Research Library
131-134. Laboratory Records
135. Laboratory Records (RC)
136. Document Reference Section
137. Research and Development Division
138-152. DTIE